Beam dynamics in insertion devices

o **Closed orbit perturbation and correction**

o **Linear optics perturbation and correction**

o **Nonlinear dynamics**

  ✥ **After sextupoles, IDs are the biggest nonlinearity at light sources and damping rings**

  ✥ **Nonlinearities from construction tolerances**

  ✥ **Nonlinearities intrinsic to insertion device design**

    ⬉ **Linearly polarized ID**

    ⬉ **End correctors**
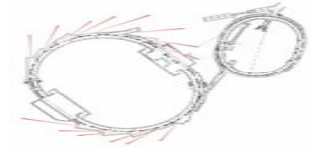
   ⬉ **Elliptically polarized ID**

What is an insertion device?

• **An insertion device has a periodic magnetic field designed to make the electron trajectory wiggle and generate intense synchrotron radiation.**

• **Wiggler and undulator IDs generate different synchrotron radiation spectra, but are essentially the same as far as beam dynamics are concerned. Undulators tend to have shorter periods and weaker fields.**

• **Used as synchrotron radiation sources, in storage ring colliders and in damping rings for linear colliders.**
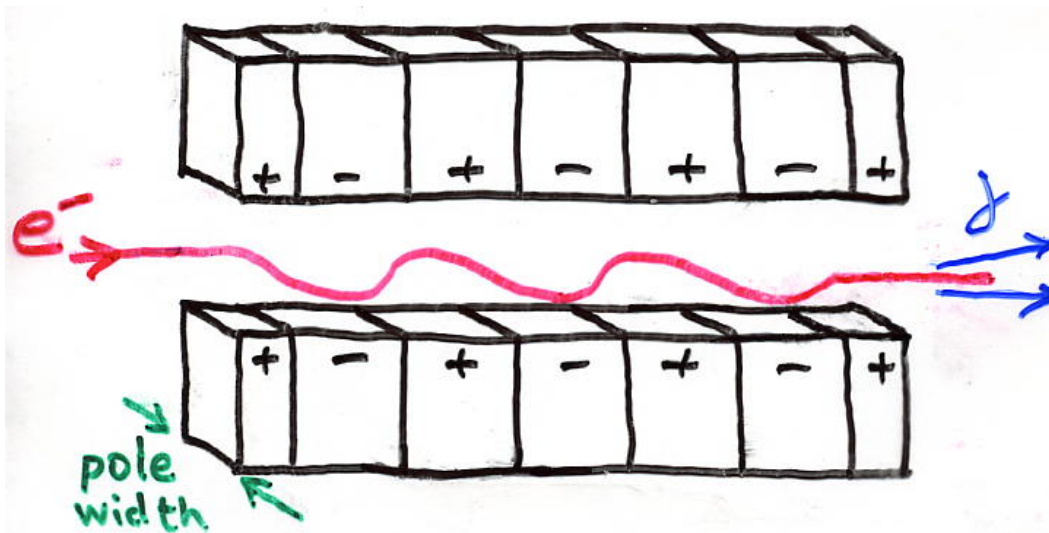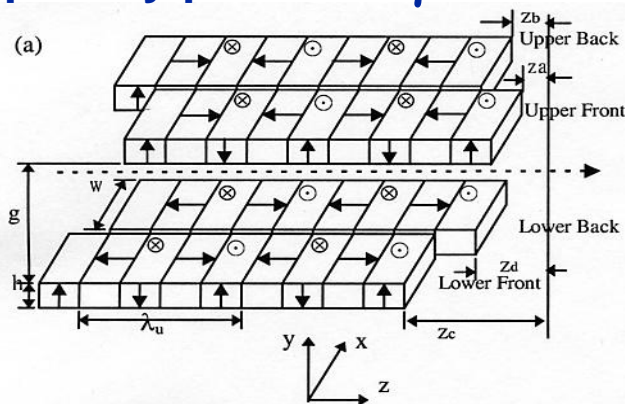
Insertion device examples

•Can be made of permanent magnets, electromagnets, or superconducting.

• Can be linearly polarized, so electrons wiggle in one plane, or elliptically polarized, so electrons travel in elliptical helixes generating elliptically polarized γs.
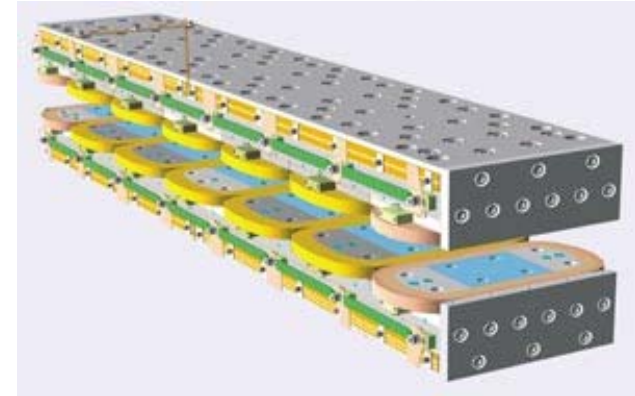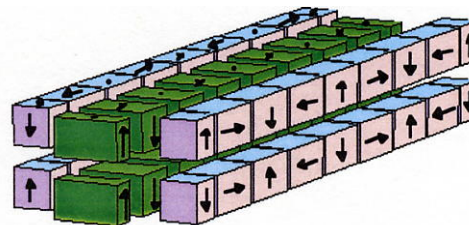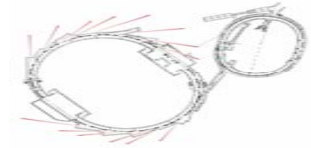
CESR superferric wiggler

Variable elliptical polarization

Figure 8 undulator

**Elettra permanent magnet ID**

Control of closed orbit

Often users adjust the spectrum from undulators by changing undulator gaps or row phase in EPUs. It's important to keep the orbit constant during these field changes to not disrupt other users. Usually use two steering magnets to correct the first and second field integrals.
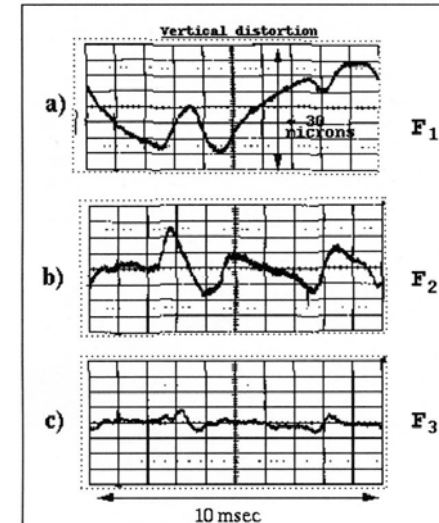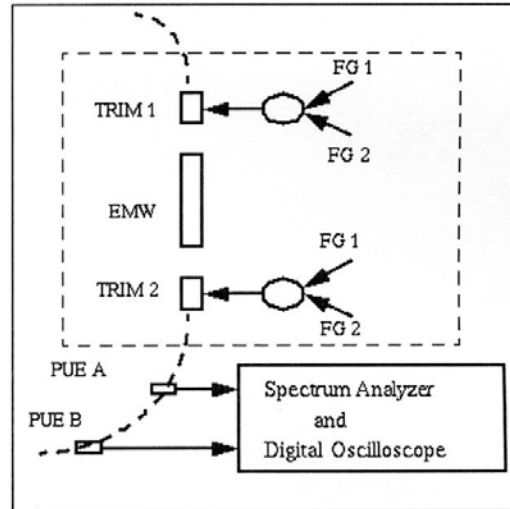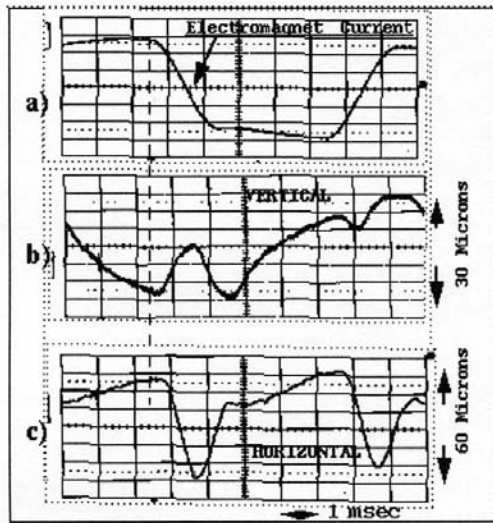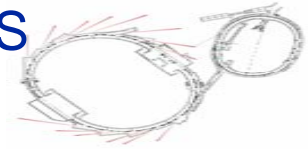
first integral
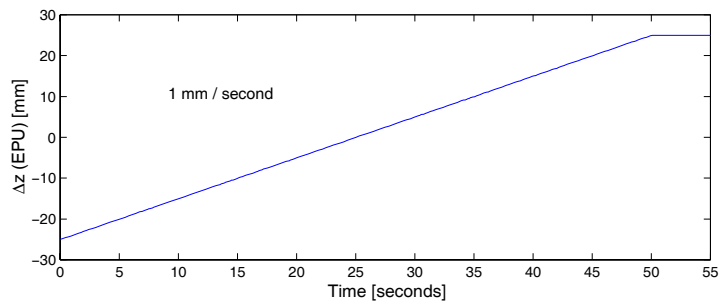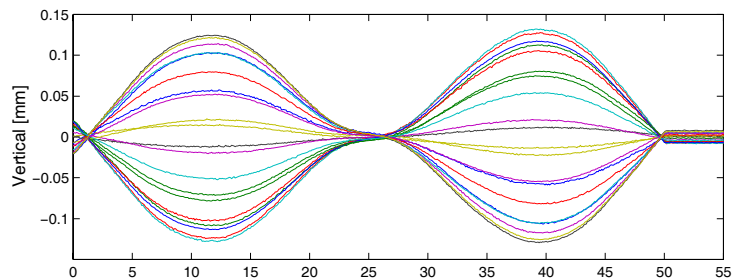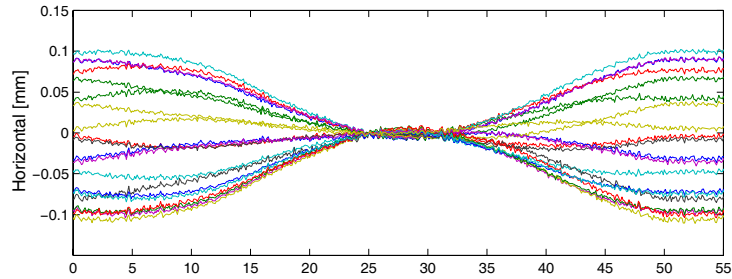
X'

corrected — **steerers**

2nd integral

X
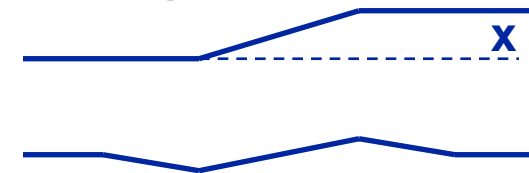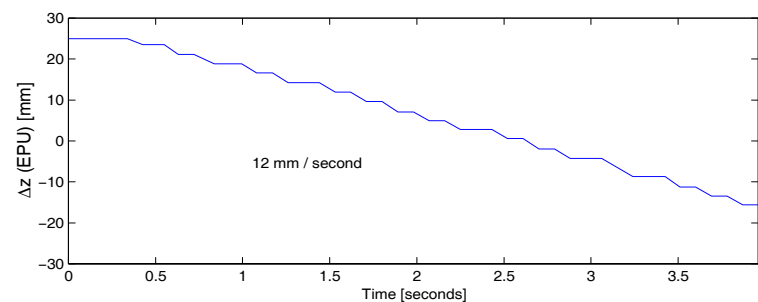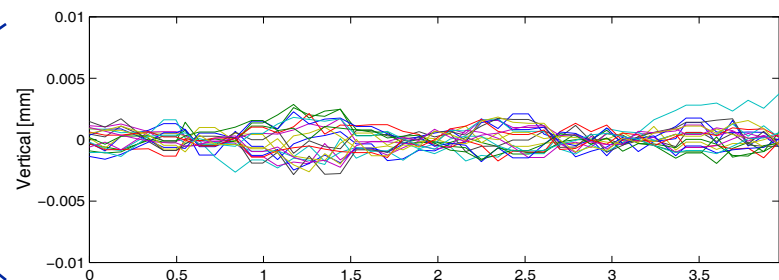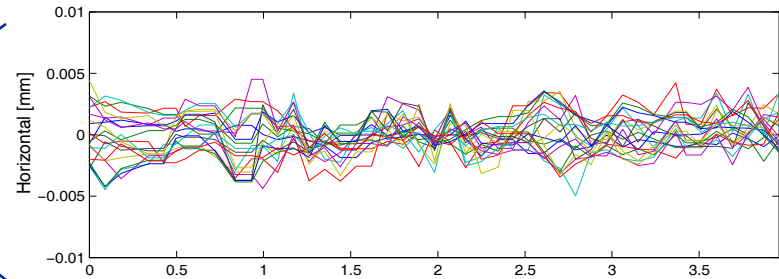
Example: EPW at NSLS switches at 100 Hz (Singh and Krinsky, PAC'97)

EPU FEED FORWARD ORBIT CORRECTION at ALS

Orbit Error without Feed Forward Correction

100 Hz Feed Forward Correction

Implemented since 2000

C. Steier

Fields in insertion devices

The fields in wigglers must satisfy Maxwell's equations in free space:

$$\vec{B} = \nabla \Phi_B \qquad (\Rightarrow \nabla \times \vec{B} = 0)$$

$$\nabla^2 \Phi_B = 0 \qquad (from \; \nabla \cdot \vec{B} = 0)$$

The ID is periodic in z, so let $\quad \Phi_B = f(x,y) \cos kz$

A real ID has higher longitudinal harmonics, $\sim \cos nkz \, , \, n = 1,3,5\ldots$
but the simpler model is good enough for now.

$$\nabla^2 \Phi_B = 0 \quad \Rightarrow \quad \frac{\partial^2 f}{\partial x^2} + \frac{\partial^2 f}{\partial y^2} = k^2 f$$
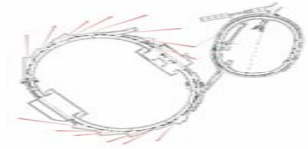
A solution is

$$f = \frac{B_0}{k_y} \cos(k_x x) \sinh(k_y y)$$

$$-k_x^2 + k_y^2 = k^2$$

The reason to choose this particular solution is …
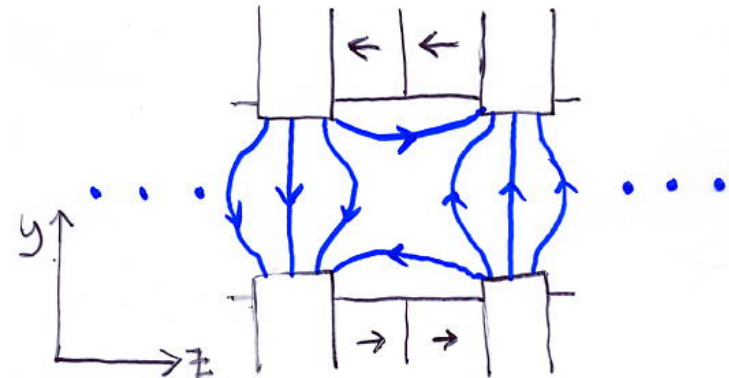
Fields in insertion devices, II

The resulting magnetic fields are

$$B_y = B_0 \cos(k_x x) \cosh(k_y y) \cos(kz)$$

$$B_x = -\frac{k_x}{k_y} B_0 \sin(k_x x) \sinh(k_y y) \cos(kz)$$

$$B_z = -\frac{k}{k_y} B_0 \cos(k_x x) \sinh(k_y y) \sin(kz)$$

This gives B_y dropping off with x, which is the case with most IDs, due to finite magnet pole width. It gives B_y increasing with y, approaching the magnet poles.

These fields provide a basis for describing a real linearly polarized ID. A real ID has higher harmonic components in z. In x, there is no constraint on k_x, so in general the fields can be described with a Fourier transform of the roll-off of B_y with x, with $k_y^2 = k^2 + k_x^2$ for each Fourier component.

Linear optics in IDs

IDs generate **vertical focusing** from the wiggling electron trajectory crossing B_z at an angle between the poles. This is like the vertical focusing in the end fields of a rectangular dipole magnet.
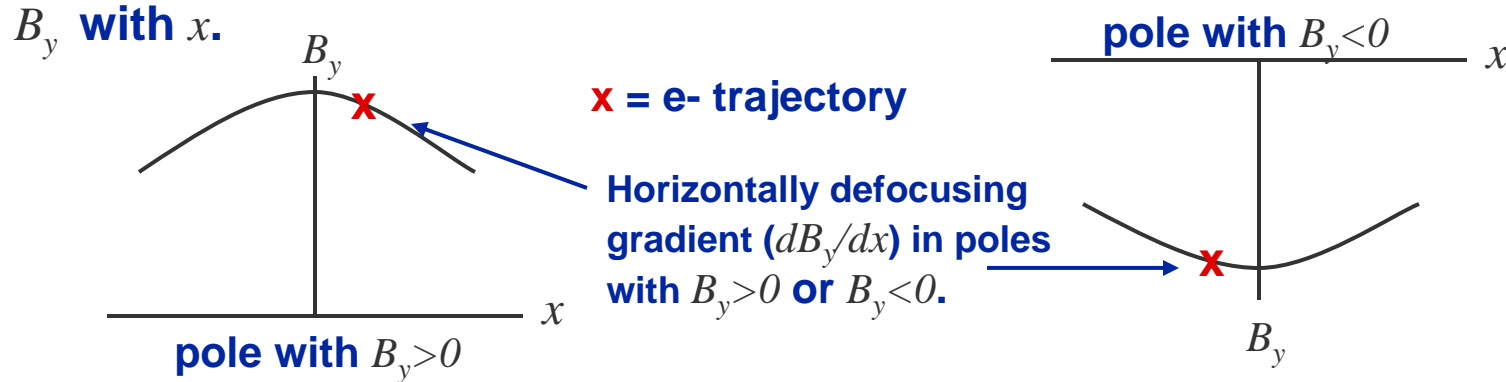

wiggling electron trajectory
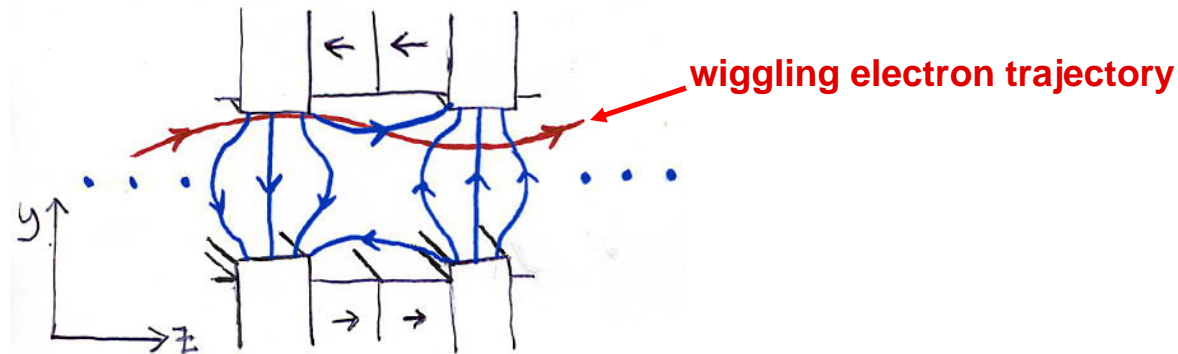
IDs generate **horizontal defocusing** (and further vertical focusing) from the wiggling electron trajectory sampling the gradient of the roll off of B_y with x.

B_y

x = e- trajectory

Horizontally defocusing gradient (dB_y/dx) in poles with $B_y>0$ or $B_y<0$.

pole with $B_y>0$

pole with $B_y<0$

x

B_y

Linear optics in IDs, II

The linear equations of motion in the wiggler fields expanded about the wiggling trajectory are[1]:

$$x'' = \frac{1}{2\rho^2} \frac{k_x^{\,2}}{k^2} x \qquad\qquad y'' = -\frac{1}{2\rho^2} \frac{k_y^{\,2}}{k^2} y$$

This linear optics perturbation causes:

1. Breaking the design periodicity of a storage ring. This can lead to degradation of the dynamic aperture.

2. Variation in beam sizes around the ring when users are changing their ID gaps. The variations can come from β function variations or coupling perturbations from skew gradients in the IDs.

The optics are corrected by adjusting quadrupoles in the vicinity of the ID as a function of the ID gap.

1.) L. Smith, LBNL, ESG Technical Note No. 24, 1986.

Linear optics correction

The code LOCO can be used in a beam-based algorithm for correcting the linear optics distortion from IDs with the following procedure:

1. Measure the response matrix with the ID gap open.

2. Then the response matrix is measured with the gap closed.

3. Fit the first response matrix to find a model of the optics without the ID distortion.

4. Starting from this model, LOCO is used to fit a model of the optics including the ID. In this second fit, only a select set of quadrupoles in the vicinity of the ID are varied. The change in the quadrupole gradients between the 1^{rst} and 2nd fit models gives a good correction for the ID optics distortion.

5. Alternatively, LOCO can be used to accurately fit the gradient perturbation from the ID, and the best correction can be calculated in an optics modeling code.
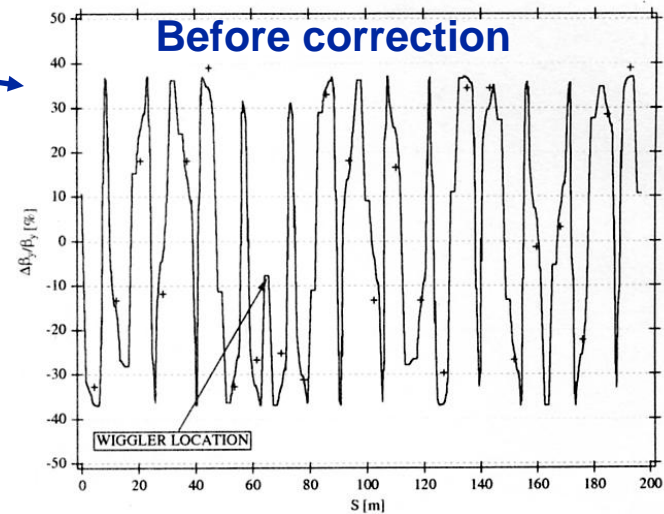
1.) L. Smith, LBNL, ESG Technical Note No. 24, 1986.
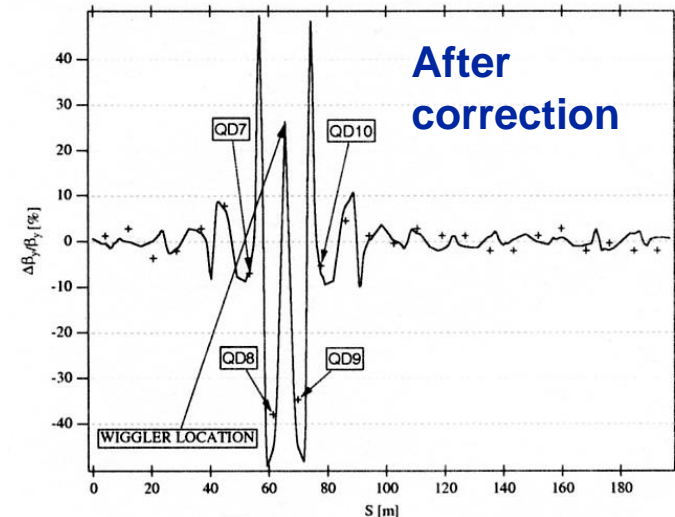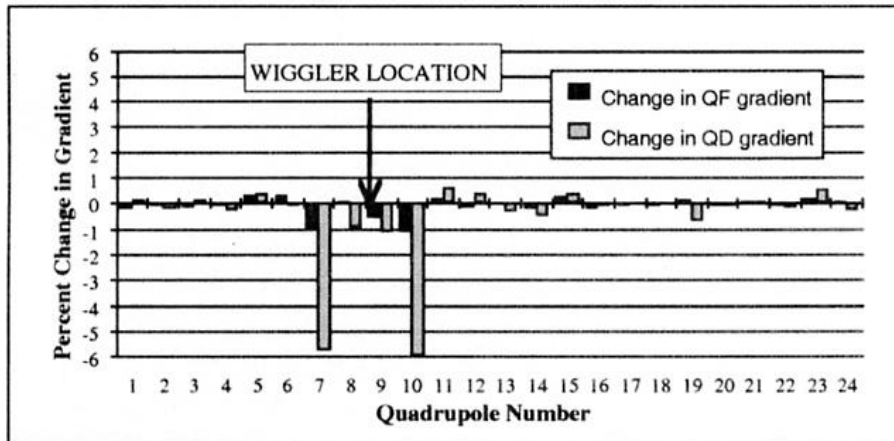
Linear optics correction at ALS

Beta function distortion from wiggler.

At ALS the quadrupoles closest to the IDs are not at the proper phase to correct optics distortions, so the optics correction cannot be made entirely local.
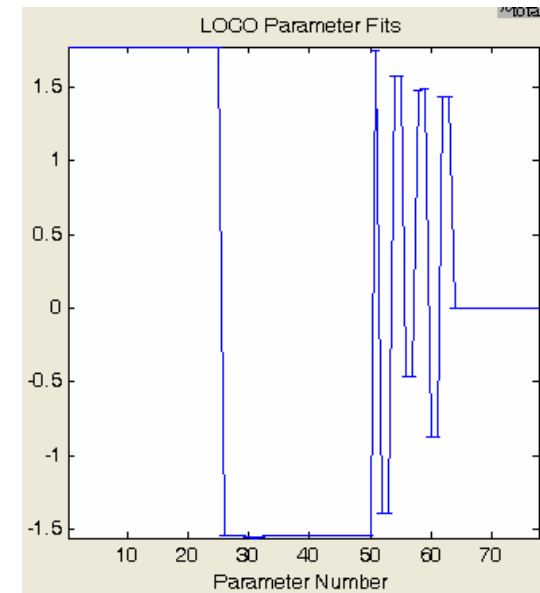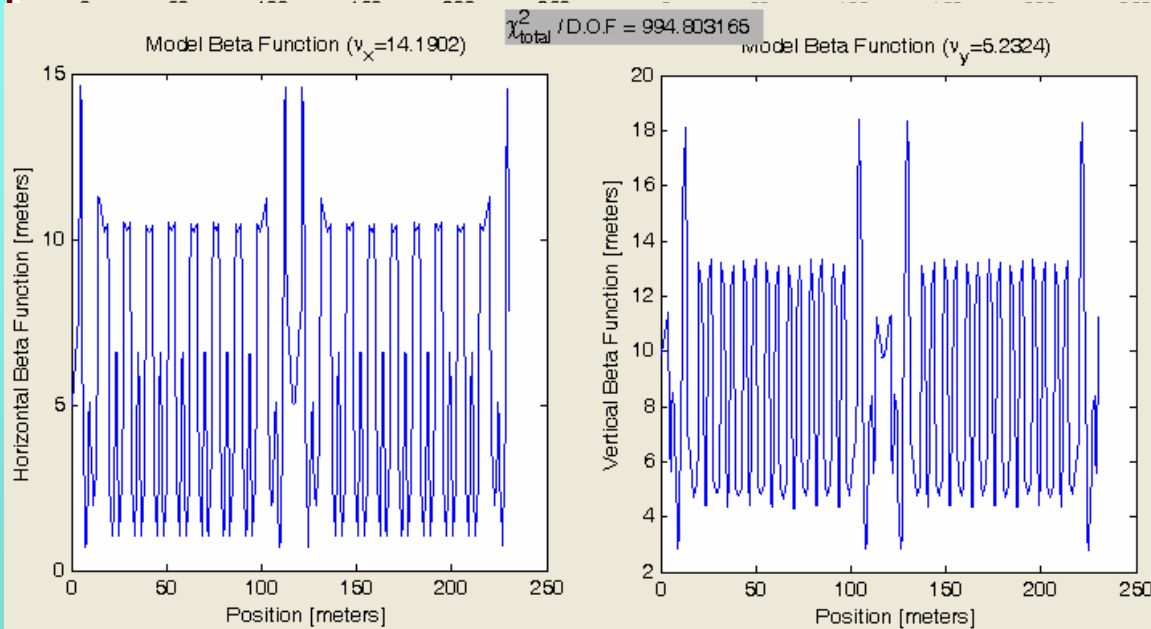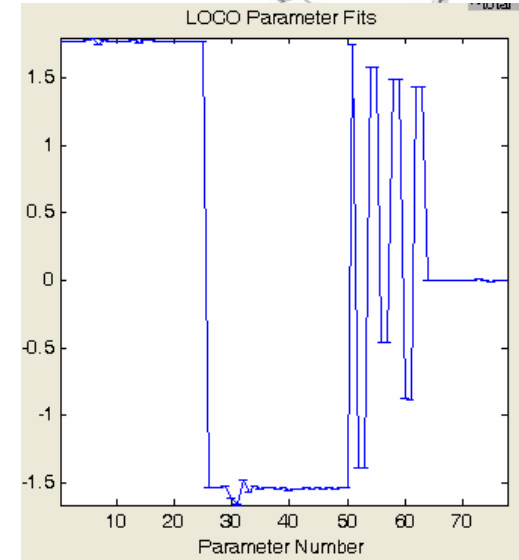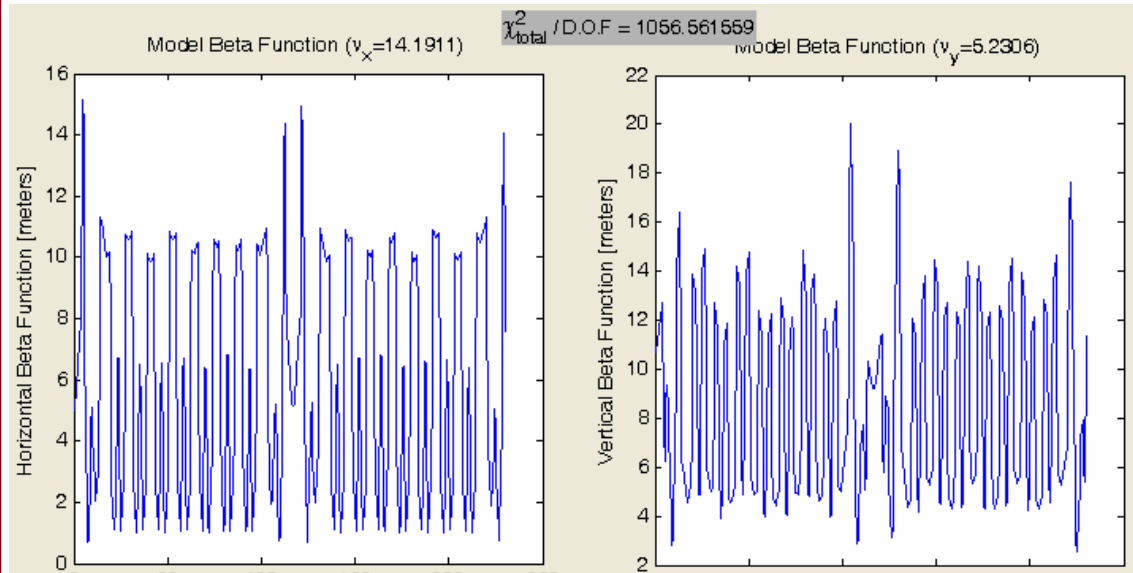
Quadrupole changes used for correction

Before correction

After correction

D. Robin et al. PAC97

Optics correction at SPEAR3

χ^2_{total} / D.O.F = 1056.561559

χ^2_{total} / D.O.F = 994.803165

AS, January 16-20, 2006, J. Safranek

Skew quadrupole compensation for ALS EPUs
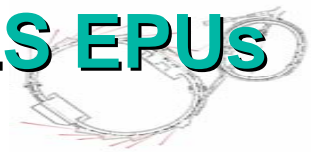
○ **Beamsize variation was solved in 2004: Installed correction coils for feedforward based compensation – routine use since June/September**

○ **Early 2005 we identified the root cause: 2-3 micron correlated motion of magnet modules due to magnetic forces**

○ **Will be able to modify design of future device such that active correction will not be necessary!**
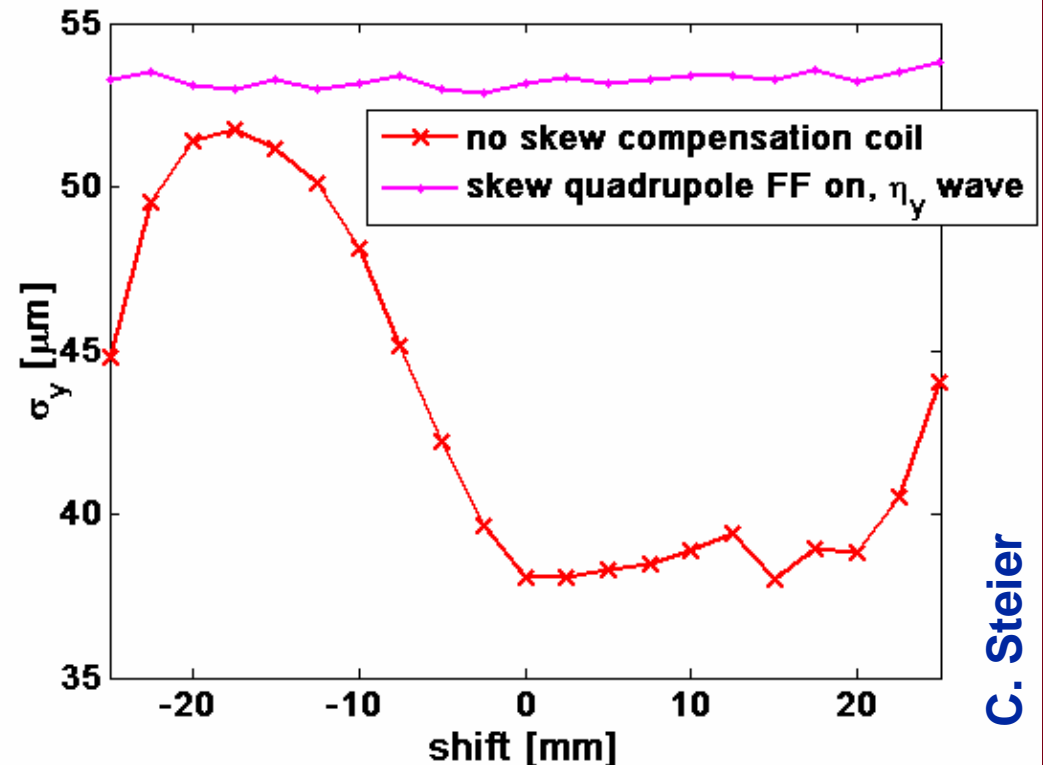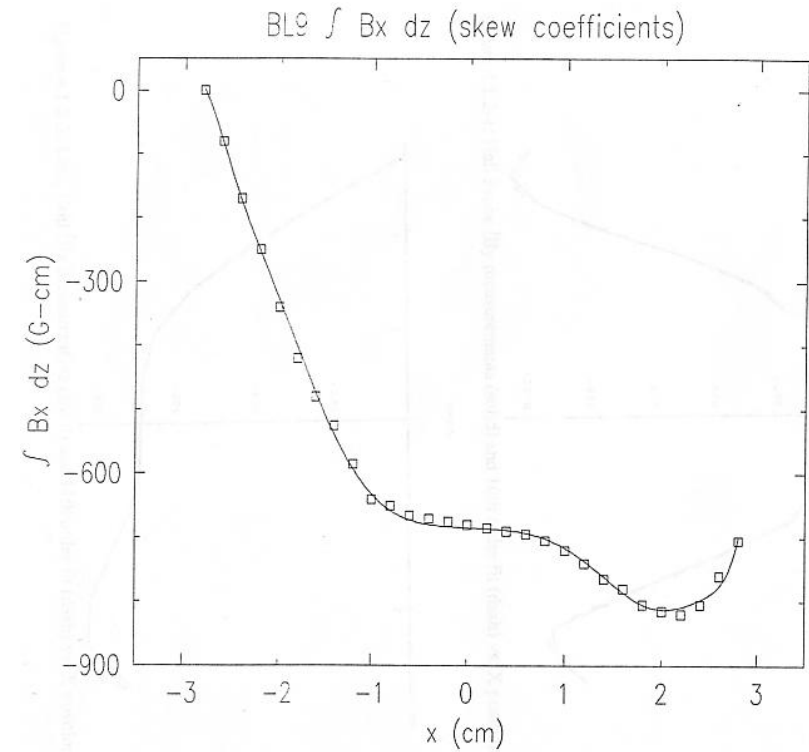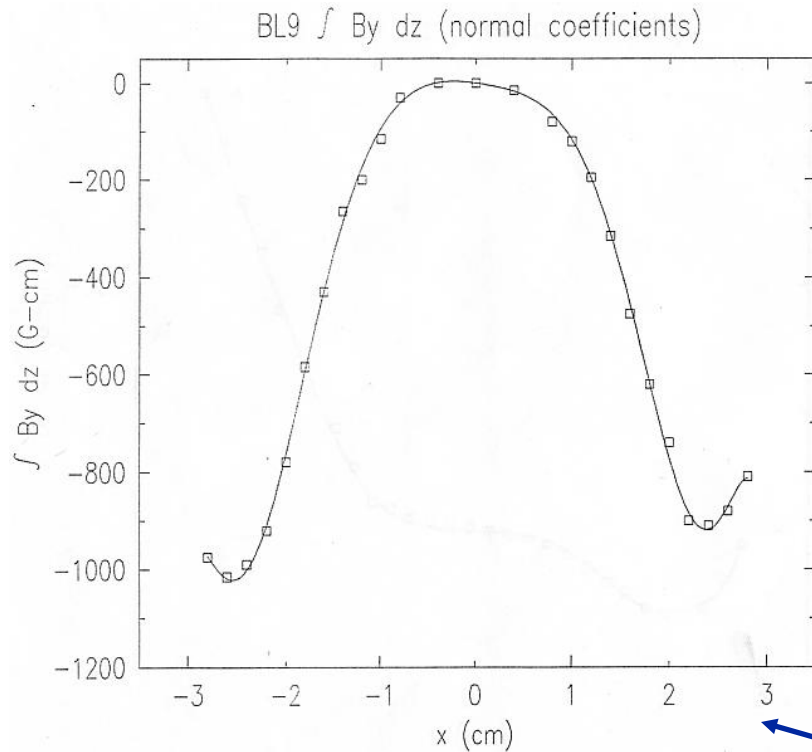

C. Steier

• **Just for reference: Whenever an undulator moves, about 120-150 magnets are changed to compensate for the effect (slow+fast feed-forward, slow+fast feedback)**

Nonlinear dynamics, construction tolerances

Example of nonlinear fields from construction tolerances, beamline 9 wiggler at SSRL:

Taylor series fit to magnetic measurements gives normal and skew multipoles.
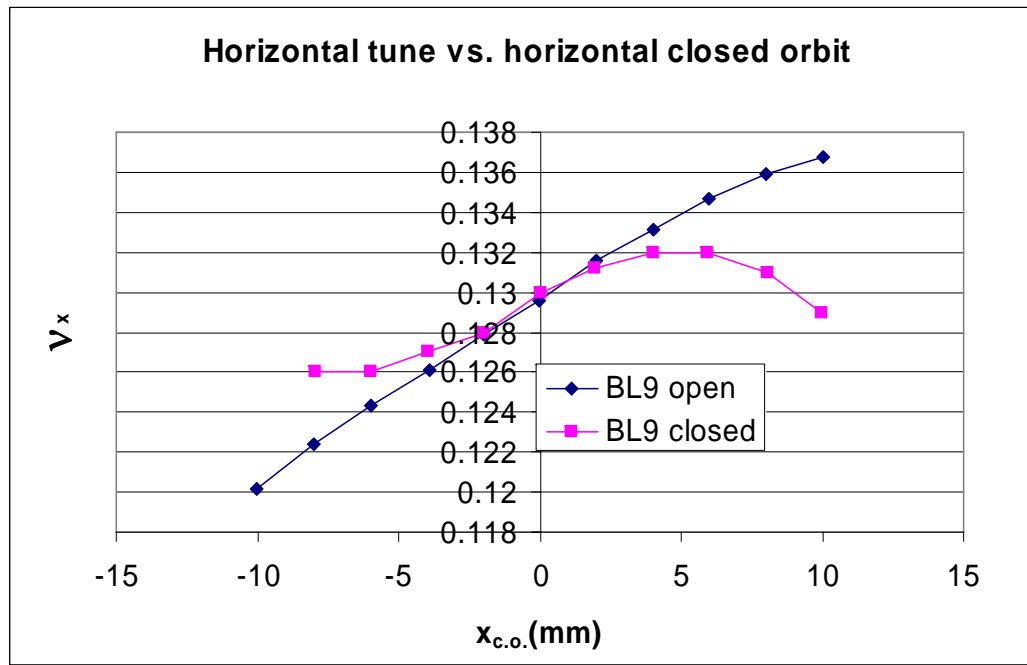
Beam-based characterization of BL9 field integrals

Measurement of tune with closed orbit bump:

$$\Delta \nu_x (x_{c.o.}) = \frac{\beta_x}{4\pi} \Delta(KL) = \frac{\beta_x}{4\pi B \rho} \frac{\partial}{\partial x} \int B_y dz$$

Closed orbit, $x_{c.o}$, varied with a 4-magnet bump. To avoid systematic errors, standardize bump magnets and correct bump coefficients for ID linear focusing and/or use feedback to generate closed bump.

Horizontal tune vs. horizontal closed orbit

Legend:
- BL9 open
- BL9 closed

Y-axis: ν_x
X-axis: $x_{c.o.}$(mm)

Beam-based characterization of BL9 normal multipoles

The field integral derivative according to the measured tune shift can be compared to the field integral derivative from magnetic measurements:
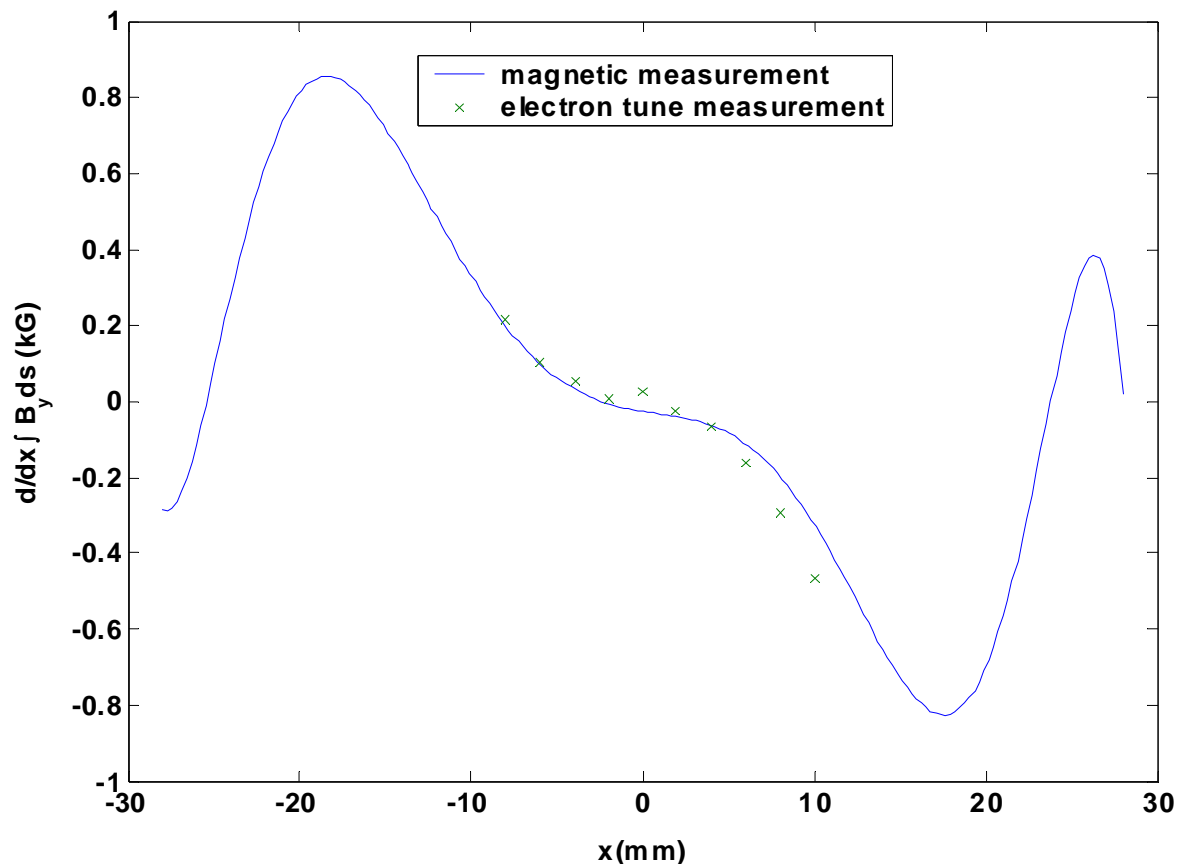

Measurement could not extend beyond +/-10 mm, for fear of melting vacuum chamber.

Beam-based method was successful in characterizing normal multipoles.

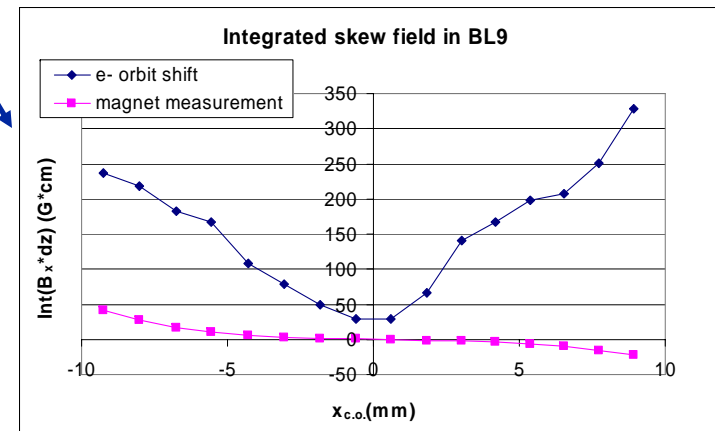# Beam-based characterization of skew multipoles
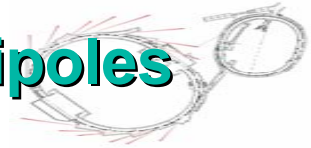
For the normal multipoles, we used tune shifts from normal gradient as a beam-based diagnostic. For skew multipoles, the skew gradient does not give such a straightforward signature as tune. Instead, the vertical orbit shift (integrated field rather than integrated gradient) can be a beam-based diagnostic.
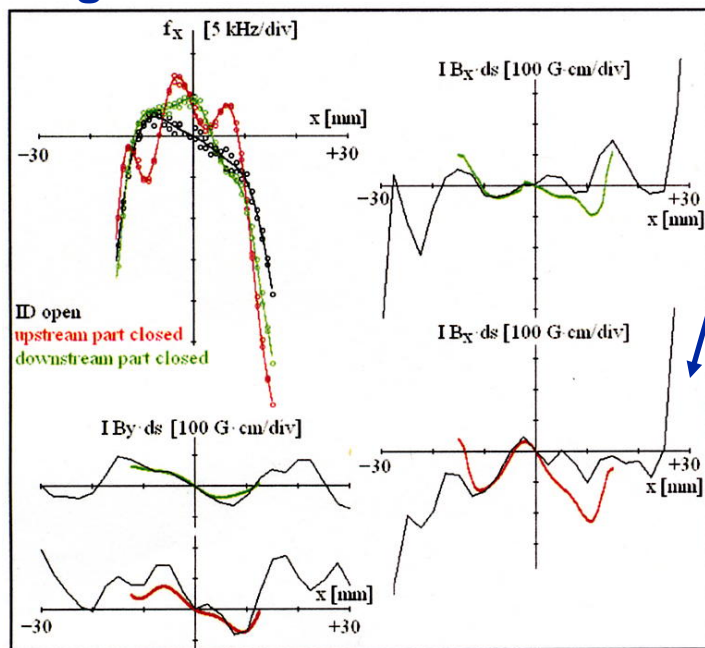
This gave reasonable results at BESSY (Kuske et al.)

Not such good results at SSRL.
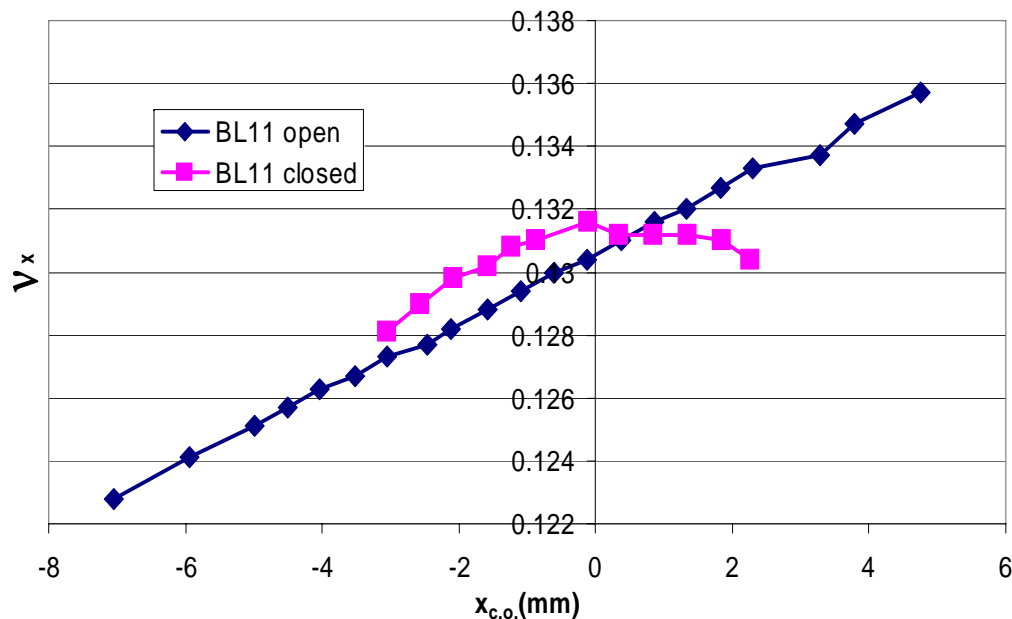

Integrated skew field in BL9

Applying LOCO to a series of orbit response matrices measured for varying closed orbit in an ID would probably give a better beam-based calibration of skew multipoles.

# Beam-based characterization of BL11 normal multipoles

The tune shift with horizontal orbit was also measured in BL11

First note that the measurements with BL11 closed extend only a couple millimeters. Due to nonlinear fields, the beam could not be stored with the orbit farther from the center. The large nonlinear fields in BL11 provided impetus for ID beam dynamics measurements at SSRL. When the device was installed in the ring at SSRL, we could no longer hold beam at the 2.3 GeV injection energy with the wiggler gap closed. At 3 GeV, the wiggler decreased the lifetime by 30% due to decrease in the dynamic aperture.

# Beam-based characterization of BL11 normal multipoles
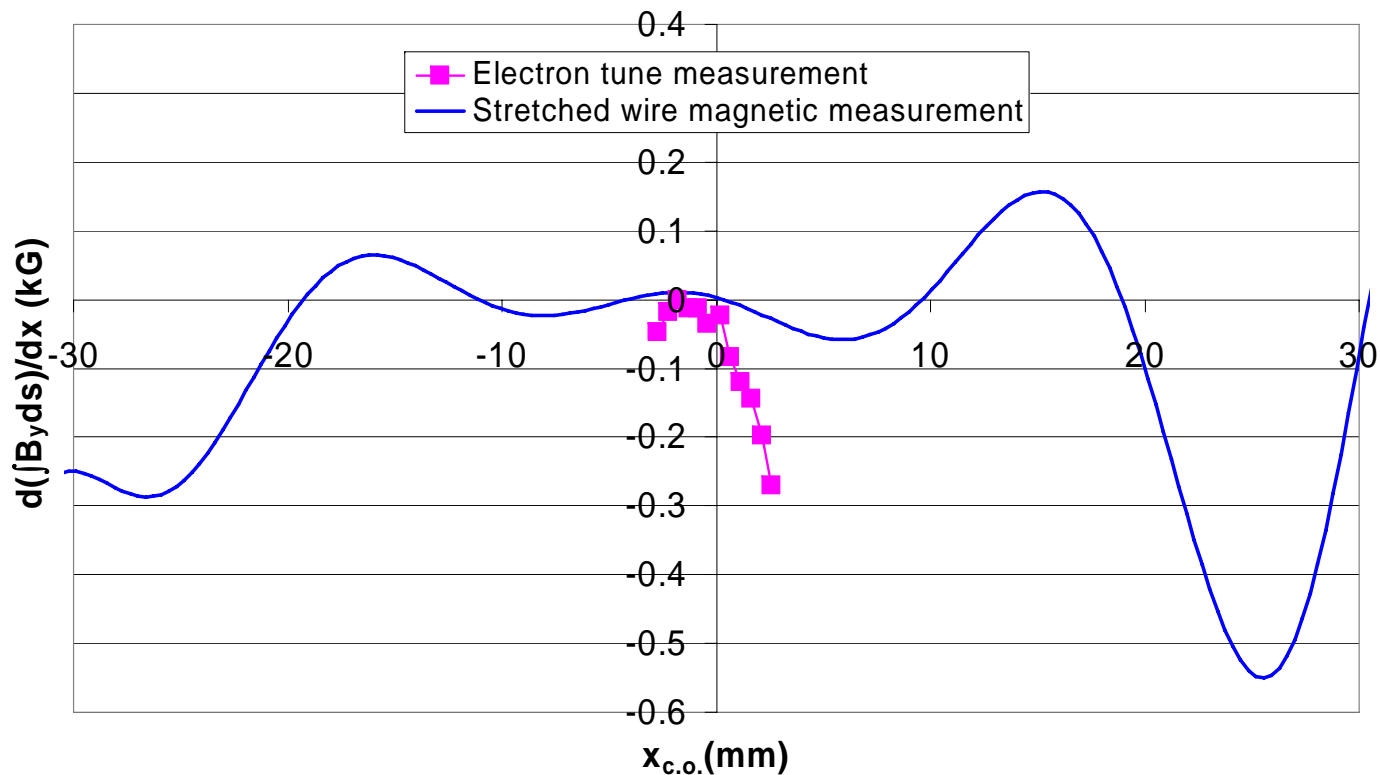
Instead of the nice agreement seen with BL9 wiggler measurements, tune measurements with BL11 indicate nonlinear fields seen by the electron beam that are not seen in magnetic measurements. The quadratic dependence of the tune with the closed orbit indicated a cubic term in the horizontal equation of motion.

# BL11 normal multipoles: tune shift with betatron amplitude

The nonlinear fields in BL11 were also characterized by kicking the beam (with an injection kicker) and digitizing the resulting betatron oscillations. NAFF was used to extract the tune vs. amplitude.

• Change in ν_x vs. x_β^2 implies strong x^3 in equation of motion

• Consistent with closed orbit bump measurement.

• Reduced maximum amplitude (BL11 closed) … reduced dynamic aperture.

• N.B. The maximum kick with all other IDs open was 245 mm², so the dynamic aperture had already been reduced by IDs prior to BL11 installation.

BL11 open
BL11 closed

ν_x

$x_\beta^2 (mm^2)$
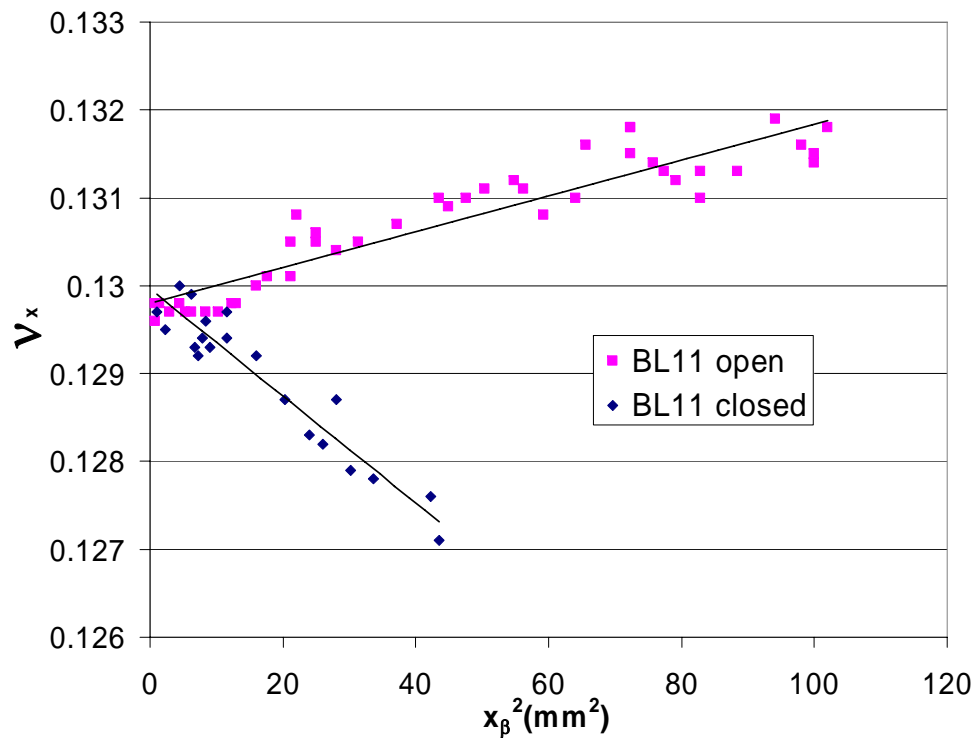
Nonlinear dynamics intrinsic to IDs
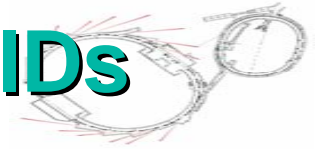
Insertion devices (IDs) can have highly nonlinear fields. Nonlinear fields seen by the electron beam come in two flavors: errors from construction tolerances and nonlinear fields intrinsic to the ID design. A linearly polarized ID has a periodic vertical field.
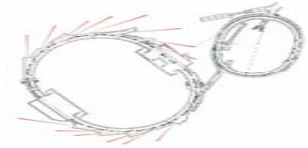
$$B_y(x, y, z) = \sum_{n=1,3,5...} B_n(x, y) \cos nkz$$

The field integral seen along a straight trajectory (i.e. as measured by a stretched wire or flip coil) is zero,

$$\int_0^{m\lambda} B_y(x, y, z)dz = 0$$

The field from one pole cancels that from the next. In a real ID, the cancellation is not perfect, due to variations in pole strengths and placement.
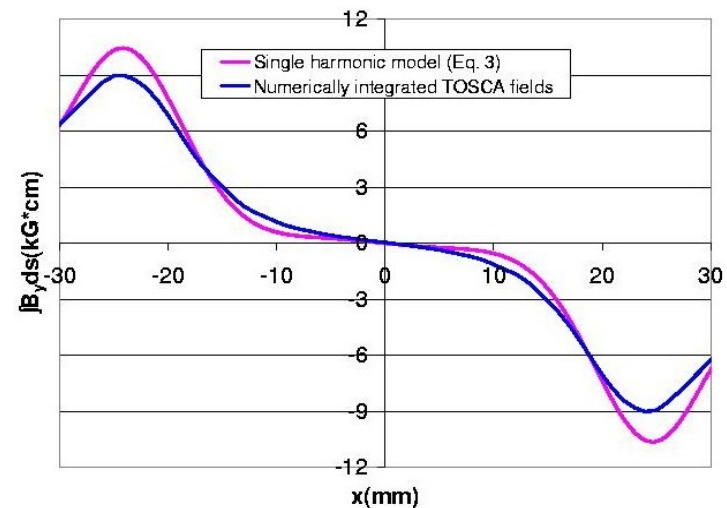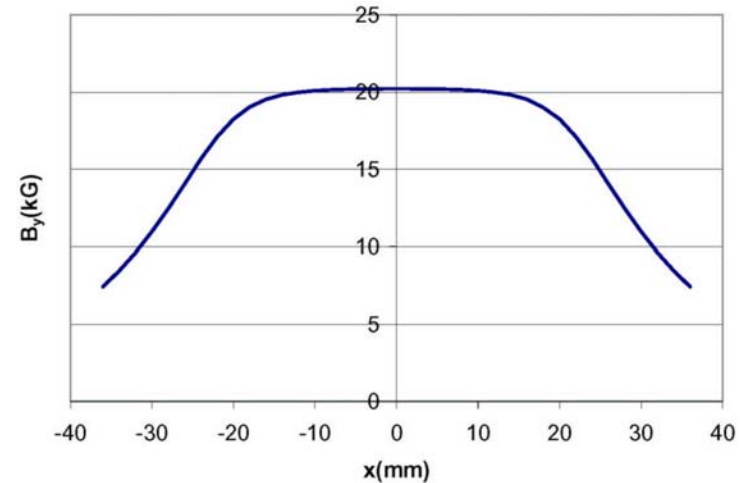
Dynamic field integrals

The field integral along a straight trajectory is zero, because the field from one pole is exactly cancelled by the next pole. Because the electron trajectory differs from one pole to the next by $2\hat{x}$, the field integral is nonzero.

$$\int B_y ds \approx \frac{-L}{2k^2 B\rho} B_y(x_i) \frac{dB_y(x_i)}{dx}$$

Dynamic field integral scales as ID period squared and as the derivative of the transverse field roll-off.

B_y(kG) vs x(mm)

- Single harmonic model (Eq. 3)
- Numerically integrated TOSCA fields

∫B_y ds(kG*cm) vs x(mm)

Nonlinear fields intrinsic to IDs: dynamic field integrals

The nonlinear fields in BL11 are only seen along the wiggling electron trajectory. To illustrate this, look at the beam dynamics in the horizontal plane only. For **y=0**, let $B_y(x,z) = B_y(x)\cos(kz)$

The beam trajectory, x_w, is given by

$$\frac{\partial^2 x_w}{\partial x^2} = \frac{B_y(x,z)}{B\rho}$$

So for an electron entering the wiggler displaced by x_i

$$x_w = x_i - \hat{x}\cos(kz), \qquad \hat{x} = \frac{B_y(x_w)}{k^2 B\rho} \quad \text{(=155μm for BL11)}$$

The integrated field seen along wiggling trajectory

$$\int B_y ds \approx \int B_y(x_i - \hat{x}\cos(kz))\cos(kz)dz$$

$$= \frac{-L}{2}\hat{x}\frac{dB_y}{dx}$$

So the integrated field seen by the electron as a function of **x** scales as the derivative of the transverse field roll-off sampled by the wiggling trajectory.

Tune shift from dynamic field integrals

The measurements of tune shift with horizontal closed orbit bump accurately predict the dynamic field integral.
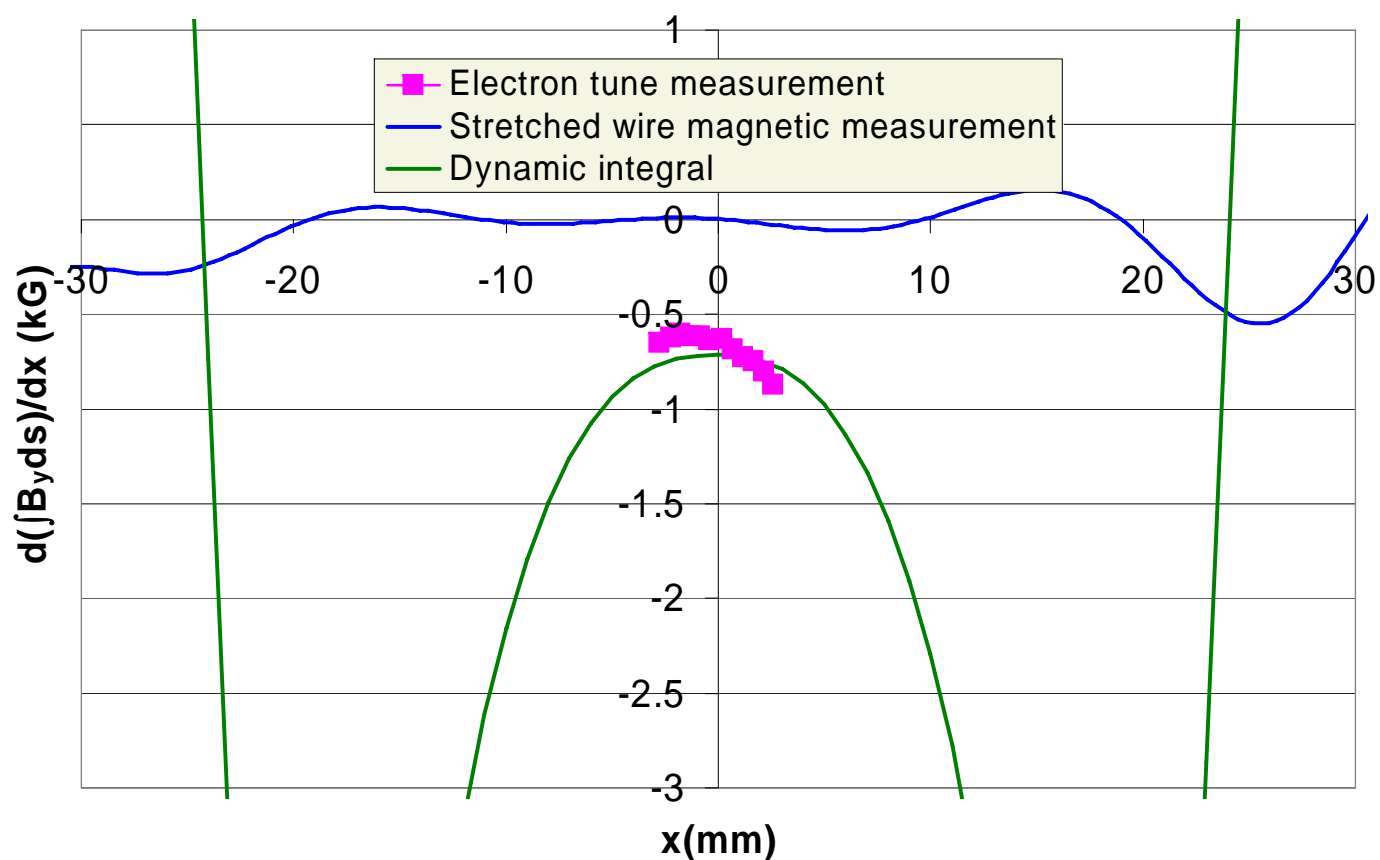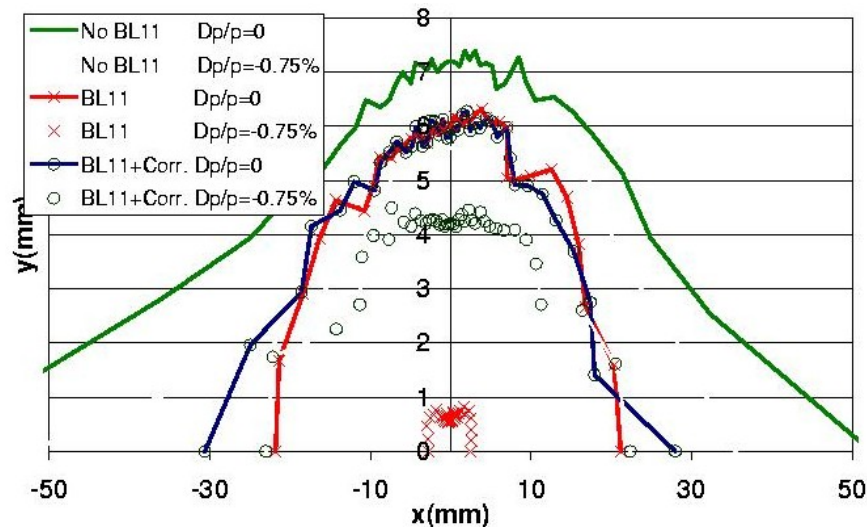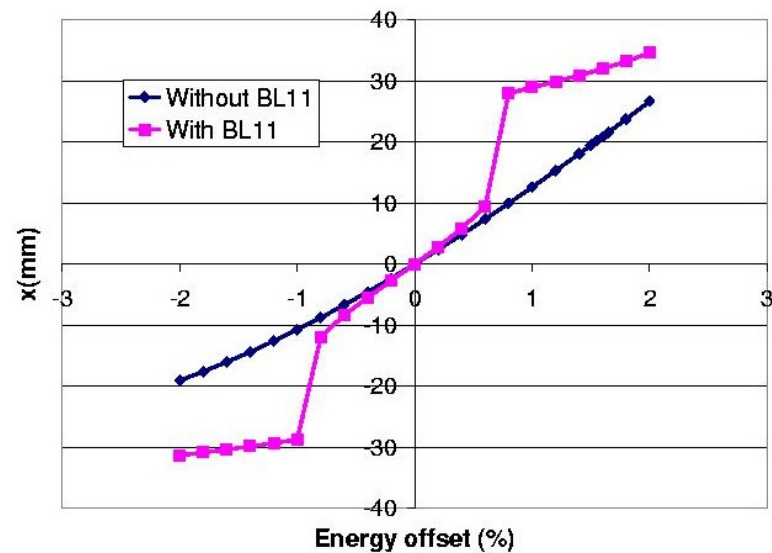
Dynamic aperture with BL11 nonlinear fields
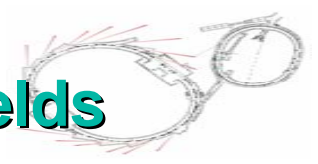
A computer code model of BL11 (with BETA) showed that the strong nonlinear fields severely distort the dispersion and limit the off-energy dynamic aperture.
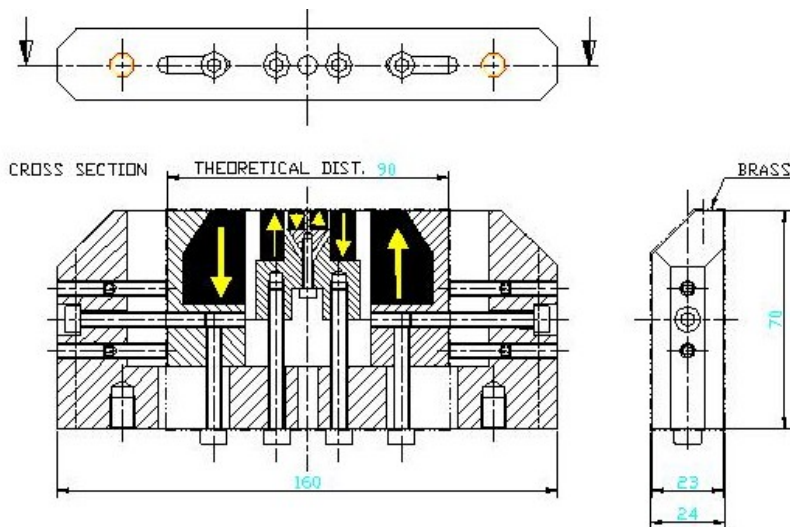
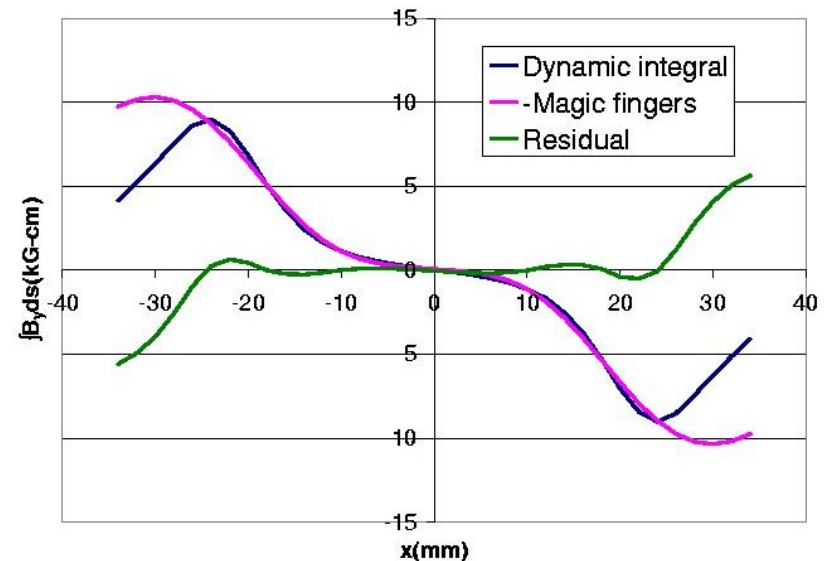This explains the reduction in lifetime and troubles with injection.

Magic finger correctors for BL11

Nonlinear corrector magnets (magic fingers) were installed at each end of the wiggler to cancel the dynamic integrals.

The bottom half of the magic fingers for one end of the wiggler. The yellow arrows indicate polarity of permanent magnets. The magnet is ~1" long.

Field integral correction achieved with magic fingers.

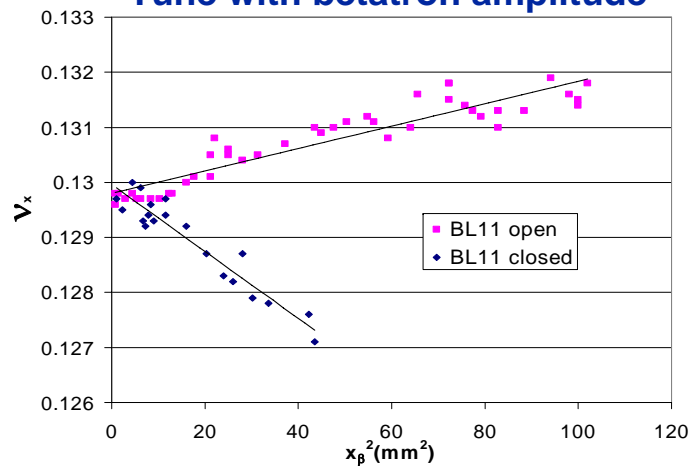# Improvement from magic fingers
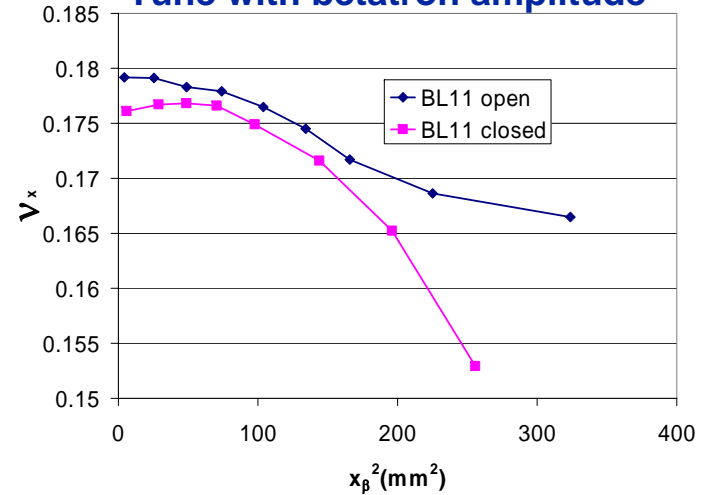
Without magic fingers:

With magic fingers:

Tune with closed orbit bump

Tune with closed orbit bump
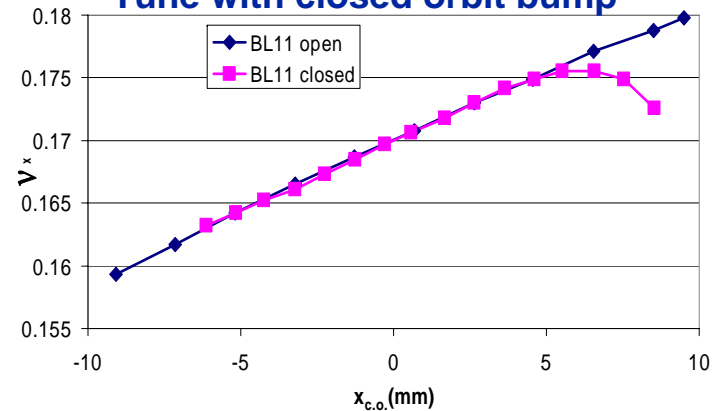
Tune with betatron amplitude

Tune with betatron amplitude

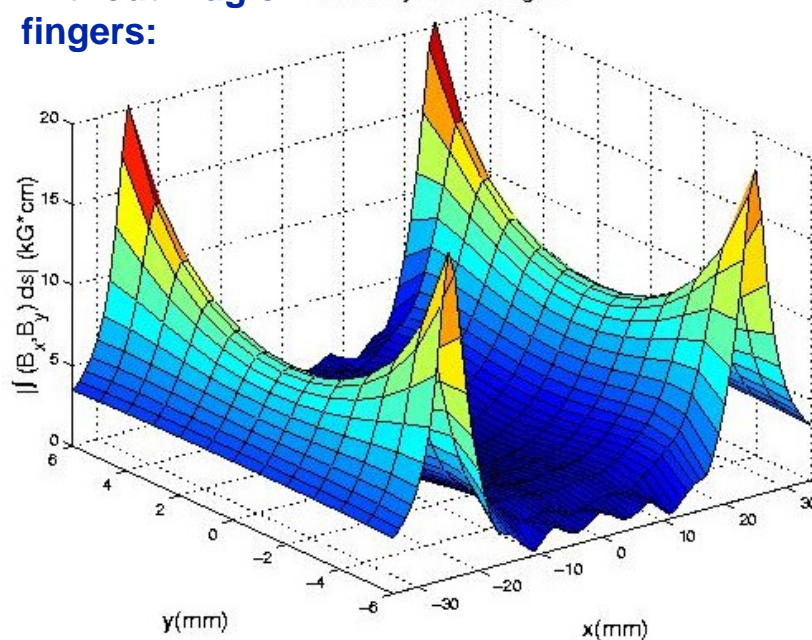# Magic finger correction imperfect

Figure shows the magnitude of the field integral from BL11 as a function of (x,y). The magnitude of the kick received by the beam passing through the wiggler is

$$|\vec{\theta}| = \frac{1}{B\rho}|\int (B_x, B_y)ds|$$

Magic fingers are thin lens multipoles, so field integrals are given by

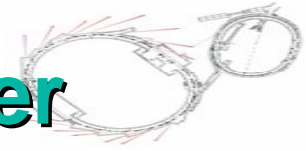$$\int (B_x + iB_y)ds = -B\rho\sum_n (b_n + ia_n)(x + iy)^{n-1}$$

The dynamic integrals do not have this form, so the magic fingers are not effective over all (x,y).

Without magic fingers:

BL11 Dynamic Integral

With magic fingers:
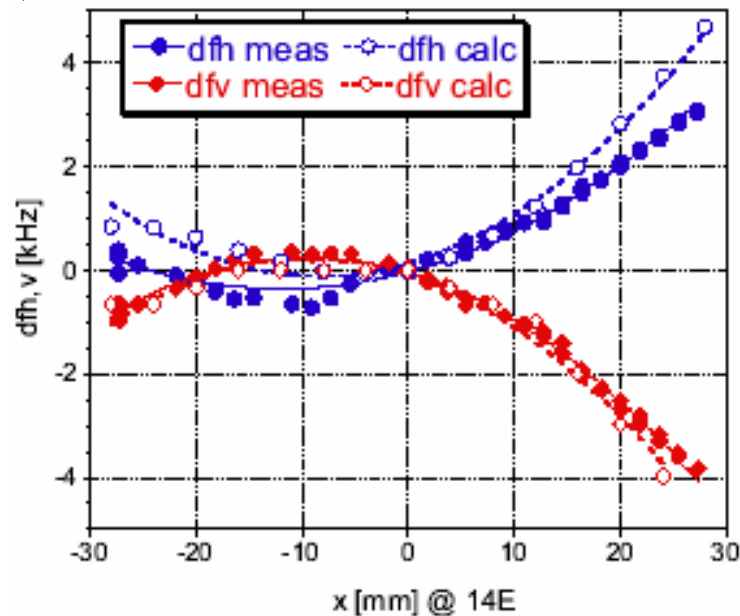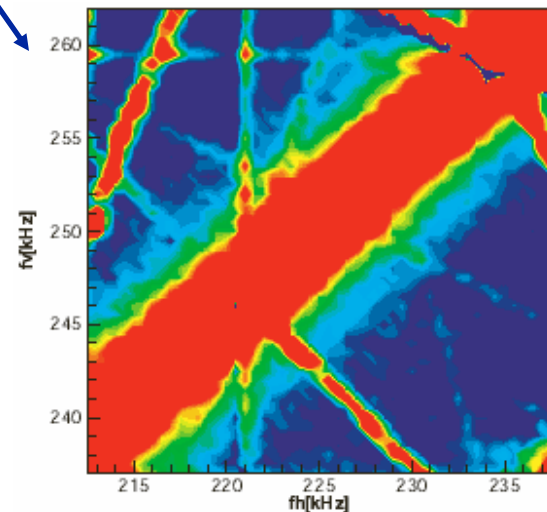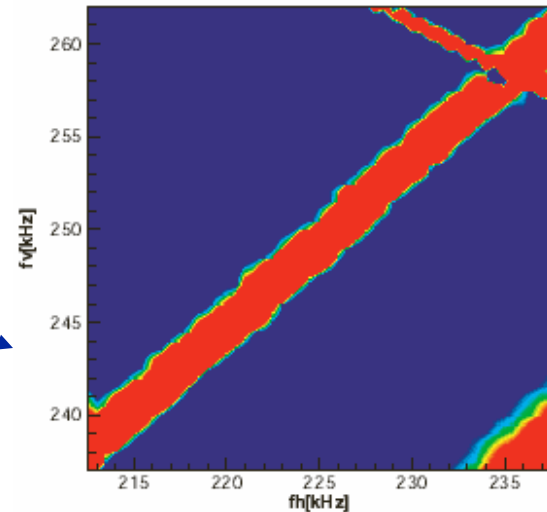
BL11 Dynamic Integral with Magic Fingers
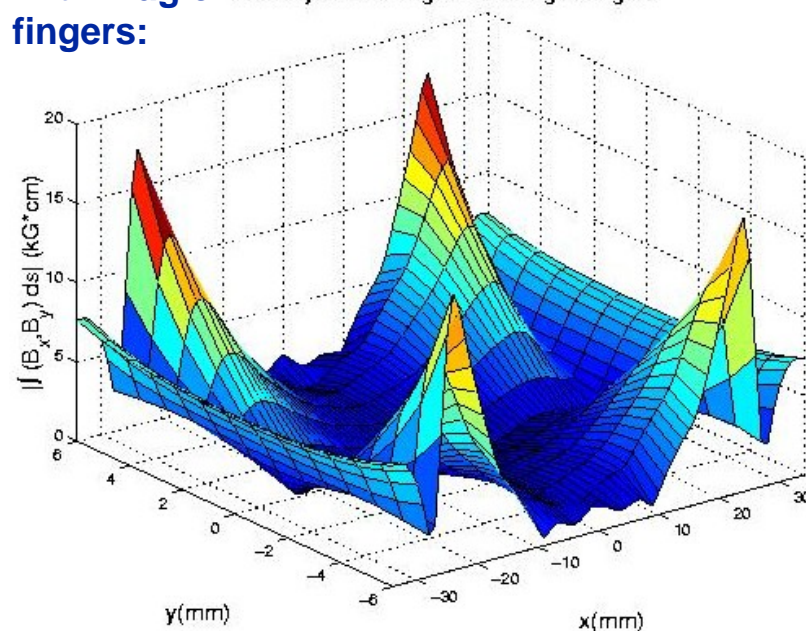
CESR superconducting wiggler

1. **Tune vs. closed orbit measurements confirmed expected field integrals.**

2. **Vertical beam size as a function of (ν_x, ν_y) shows resonances excited by wiggler.**

Wiggler off

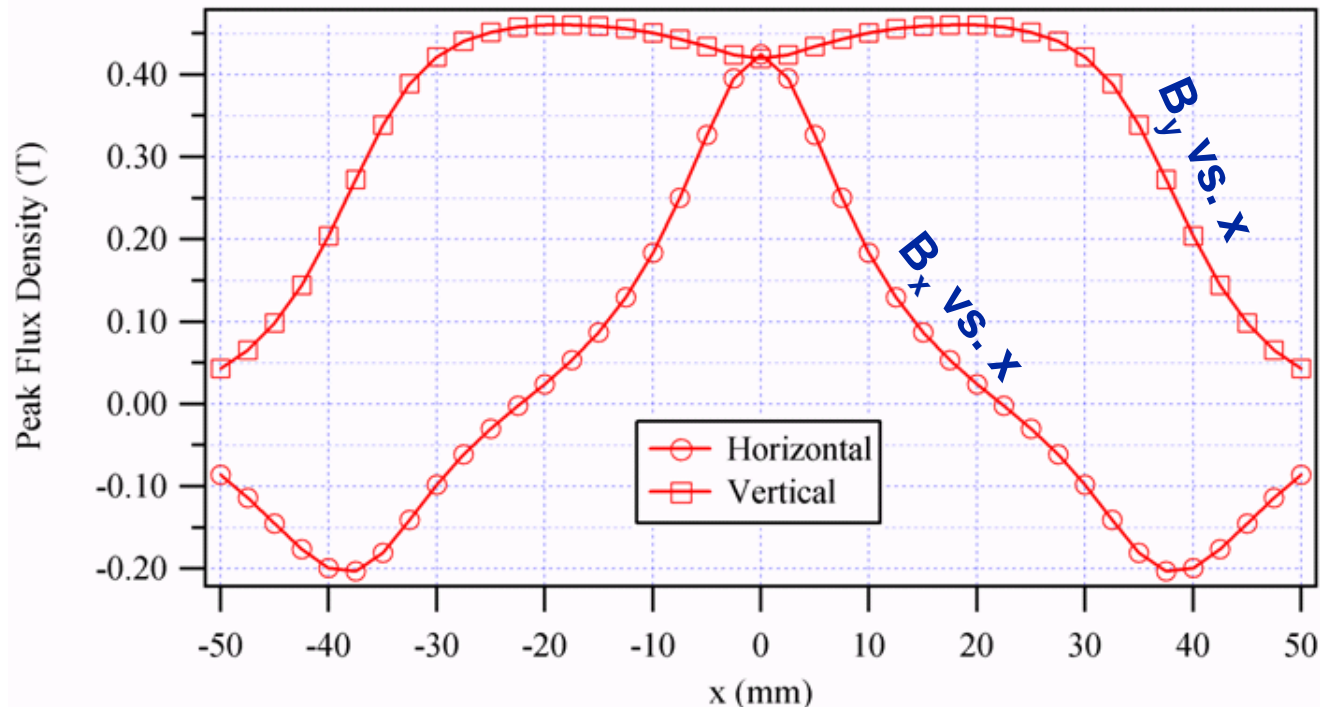**Wiggler on**

Temnykh et al., PAC03

Transverse field roll-off in 4-row EPUs

○ **Fast roll off in B_x vs. x is unavoidable.**

    ↳ **With planar IDs, wide magnet poles eliminate B_y vs. x roll-off**

    ↳ **In EPUs B_x vs. x roll-off is independent of pole width**
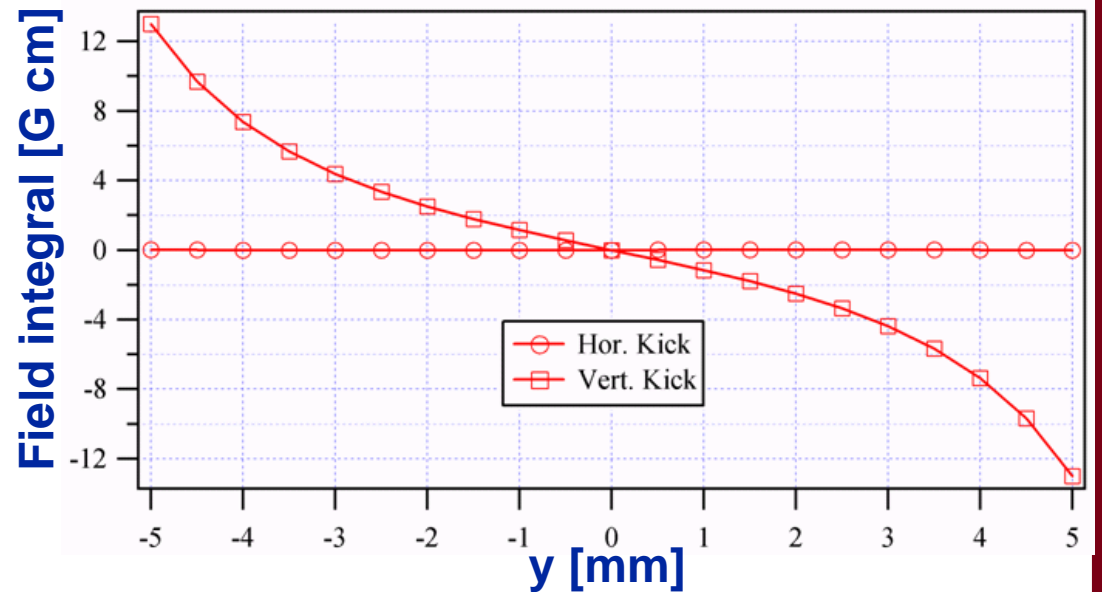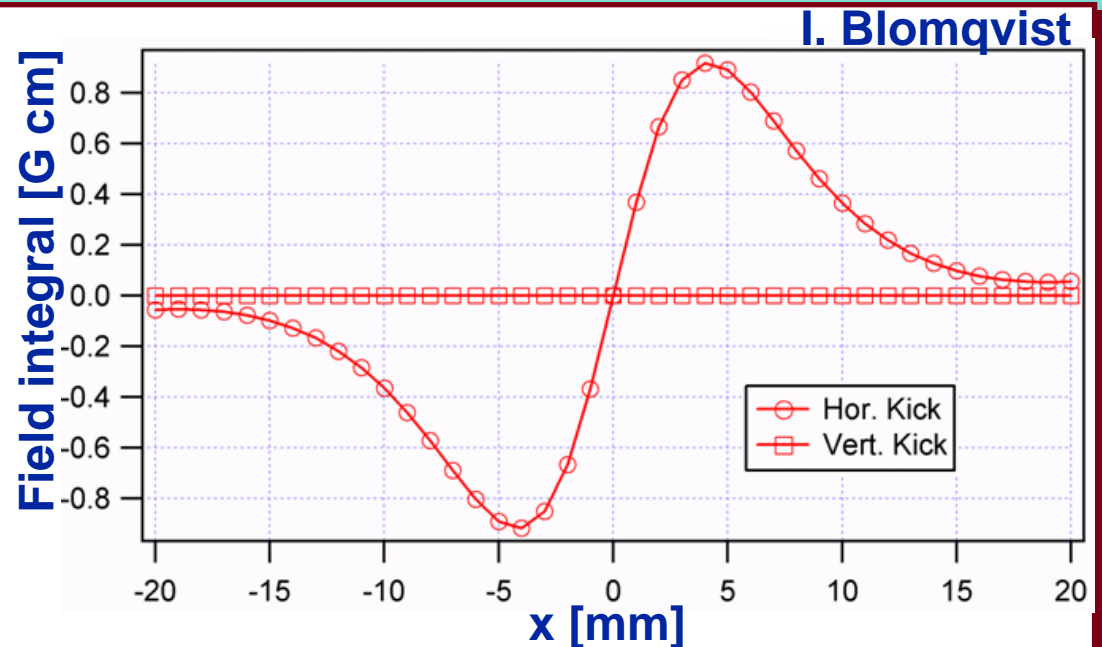
Max-lab EPU transverse field roll-off

I. Blomqvist

Figure 24. The transverse roll off for the Circular undulator phase.

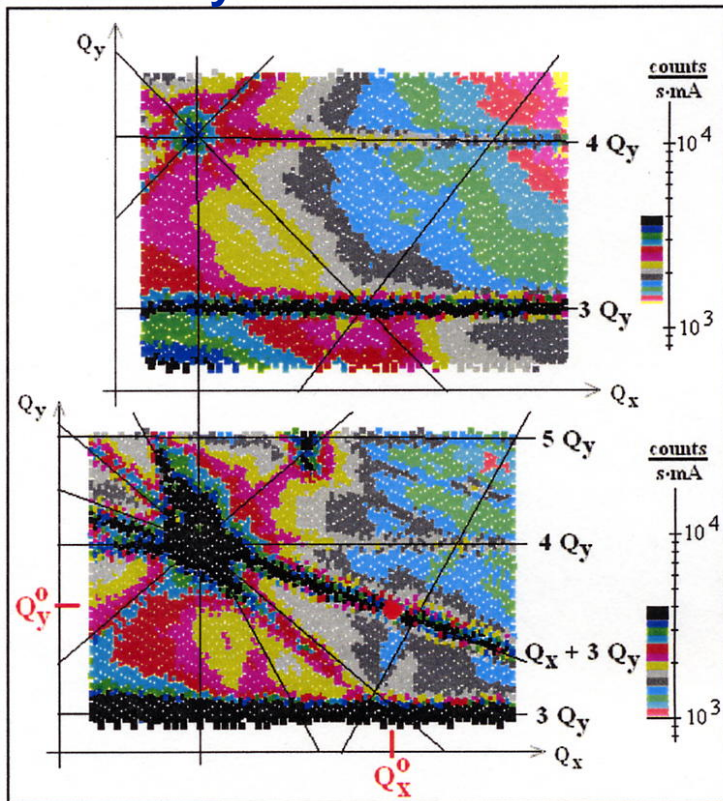# Dynamic integrals in EPUs

I. Blomqvist

- ○ **Spiraling trajectory couples with field roll-off, generating field integrals.**

- ○ **Field integrals vary with row phase and ID gap, so fixed-field nonlinear correctors would not help.**
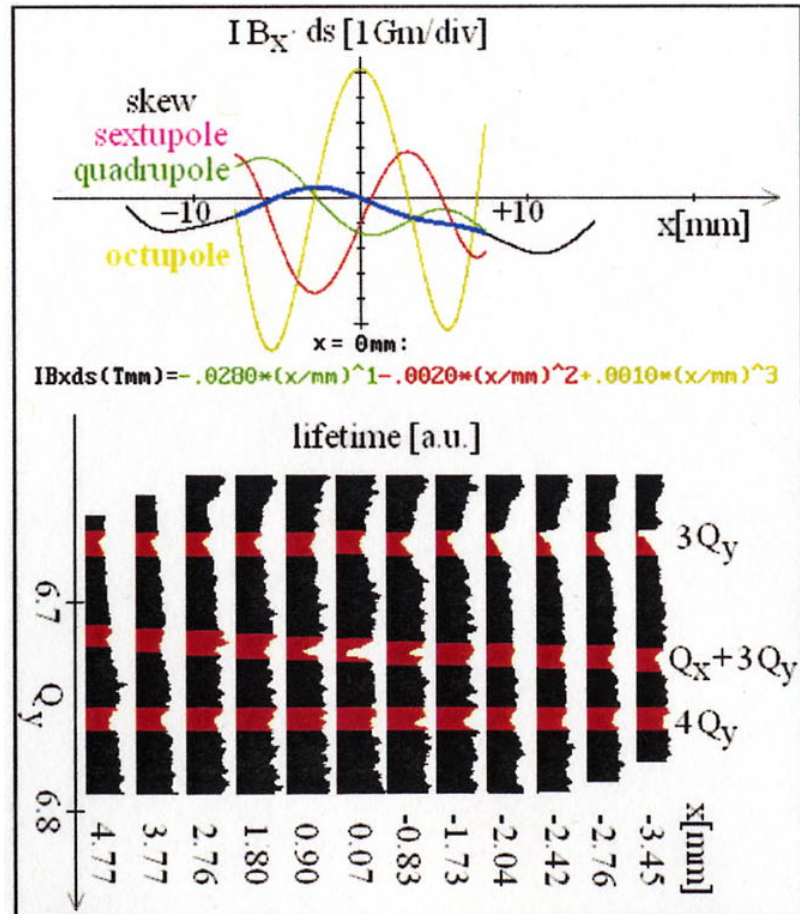
Bessy II measurements with EPUs (before shims)

Tune scans with beam loss monitor measurements can be used to identify resonances excited by IDs.

Kuske, Gorgen, Kuszynski, PAC'01

Scanning both tune and closed orbit while measuring lifetime gives a measure of multipole strengths vs. orbit.

$IBxds(Tmm) = -.0280*(x/mm)^1 - .0020*(x/mm)^2 + .0010*(x/mm)^3$

More BESSY II measurements

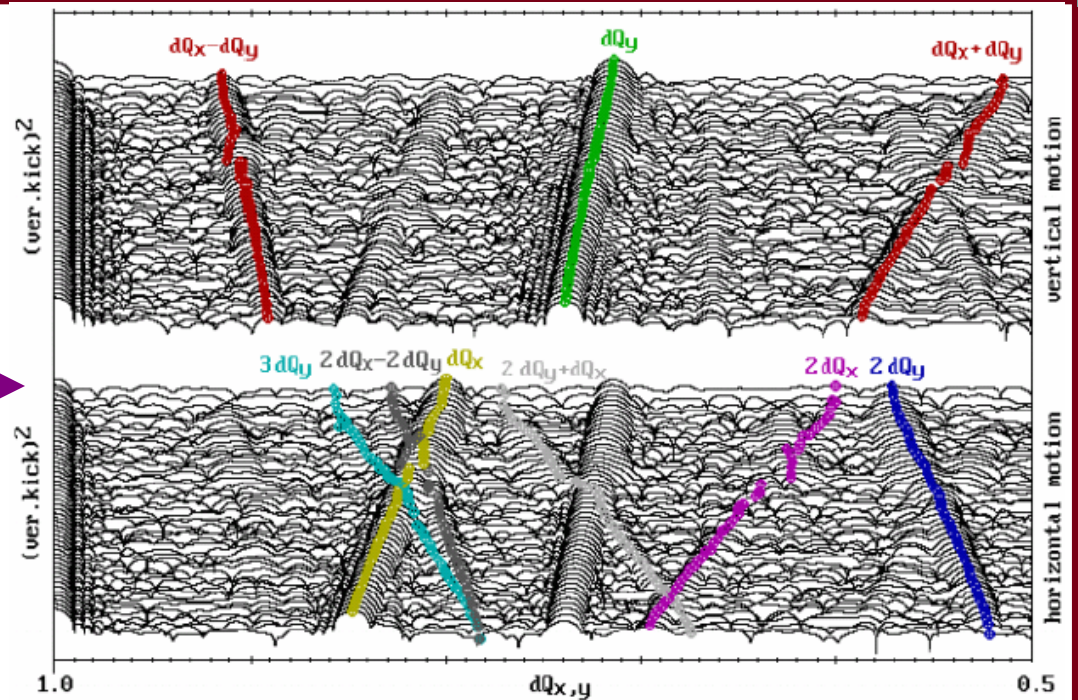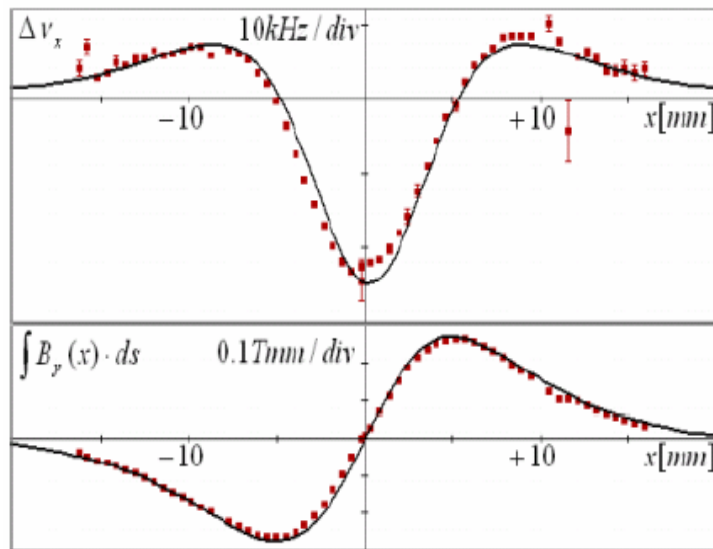○ **Resonance excitation seen in turn-by-turn BPM data.**

Figure 1: Spectra of the vertical and horizontal beam motion (top and bottom) with the fundamental tunes: dQ_x (yellow), dQ_y (green) and combinations of them.
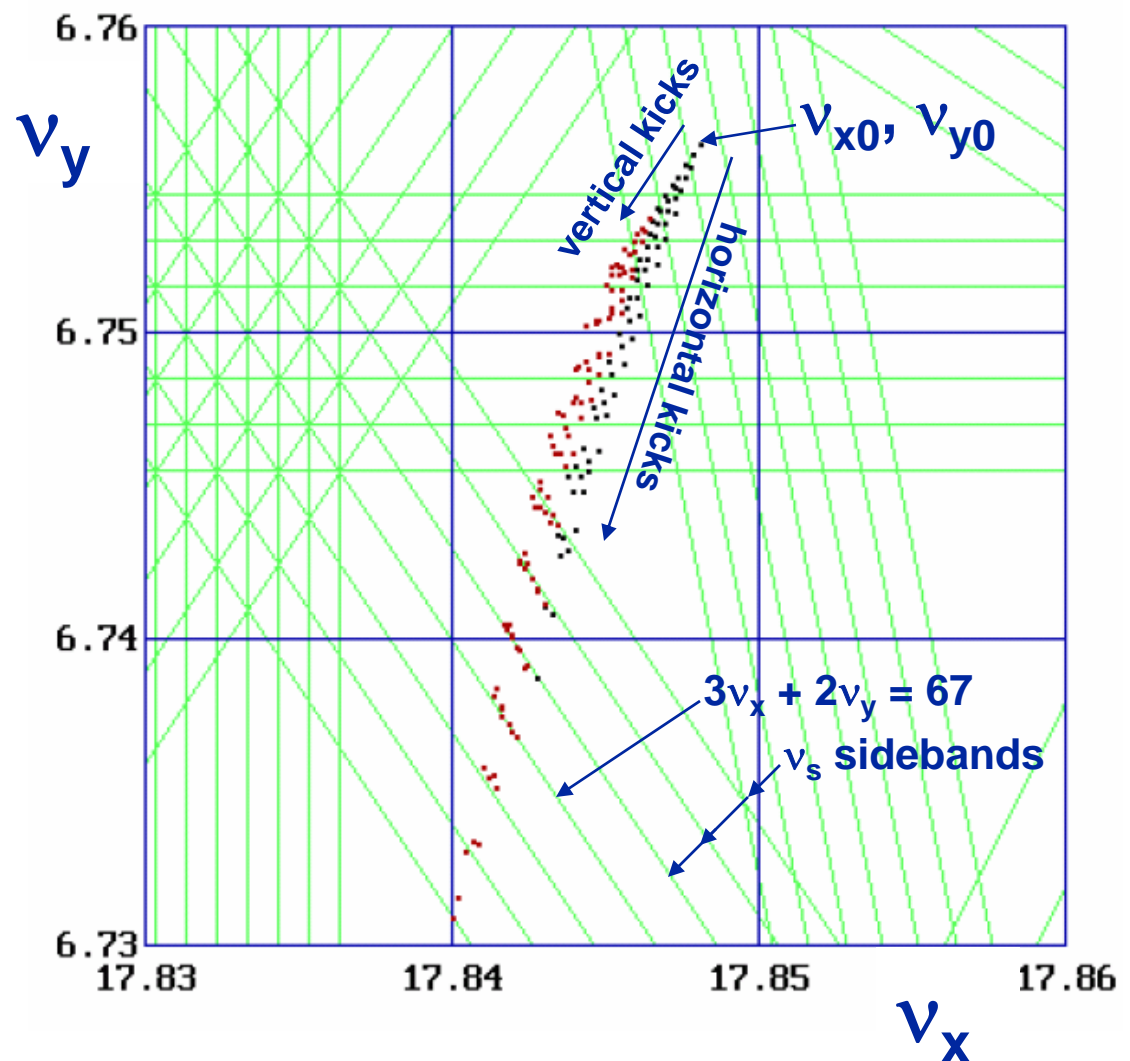

○ **Tune measurements vs. closed orbit bump confirm expected dynamic field integrals.**

Frequency map measurements at BESSY-II

○ **Frequency maps have been used to characterize EPU nonlinearities at BESSY-II.**

ν_y

vertical kicks

horizontal kicks

ν_{x0}, ν_{y0}

$3\nu_x + 2\nu_y = 67$
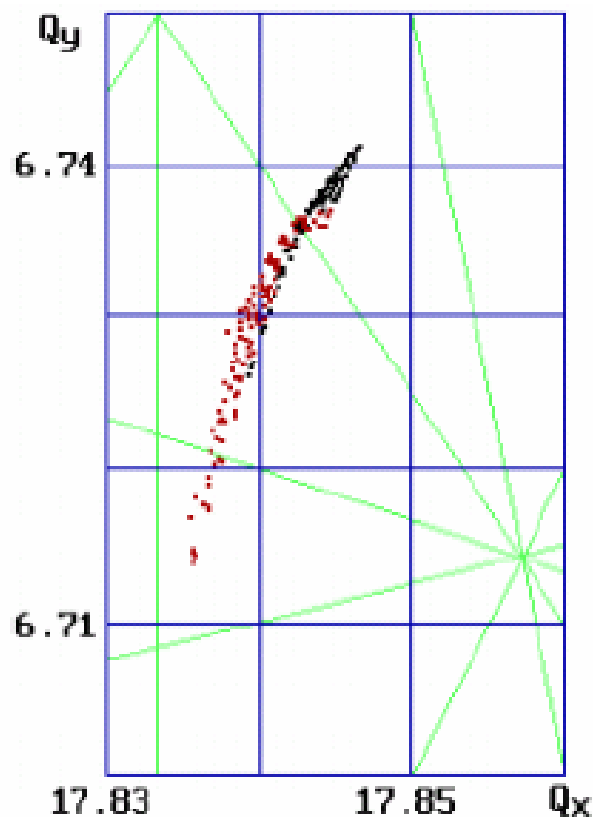
ν_s **sidebands**

ν_x

Frequency map measurements at BESSY-II
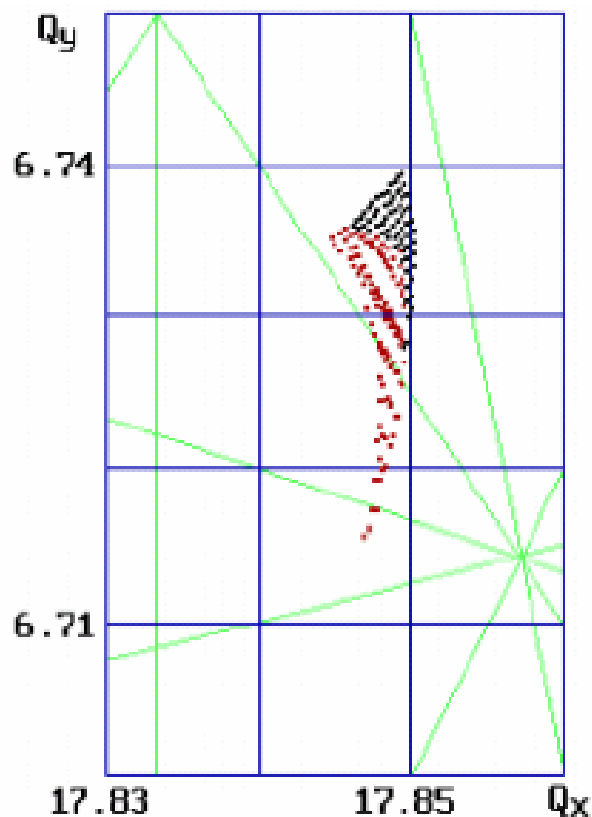
- Beam dynamics highly dependent on EPU row phase.
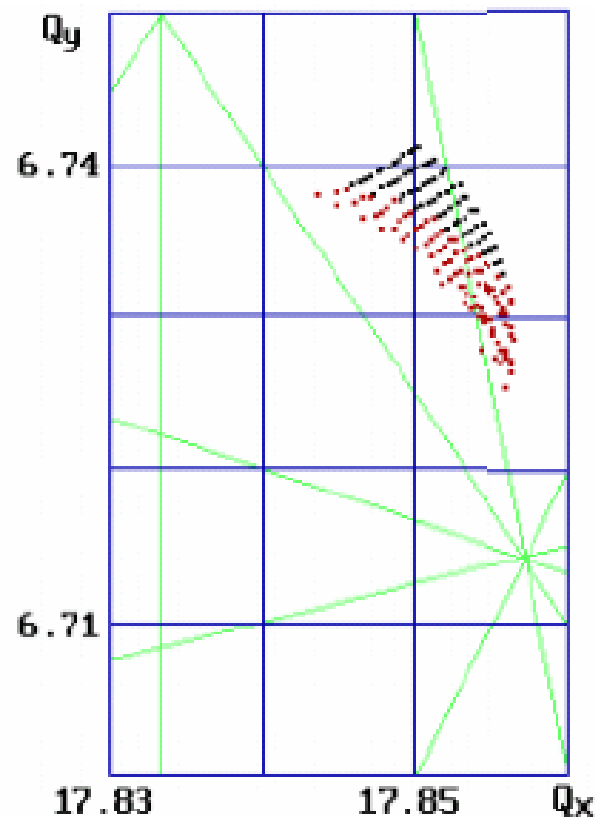
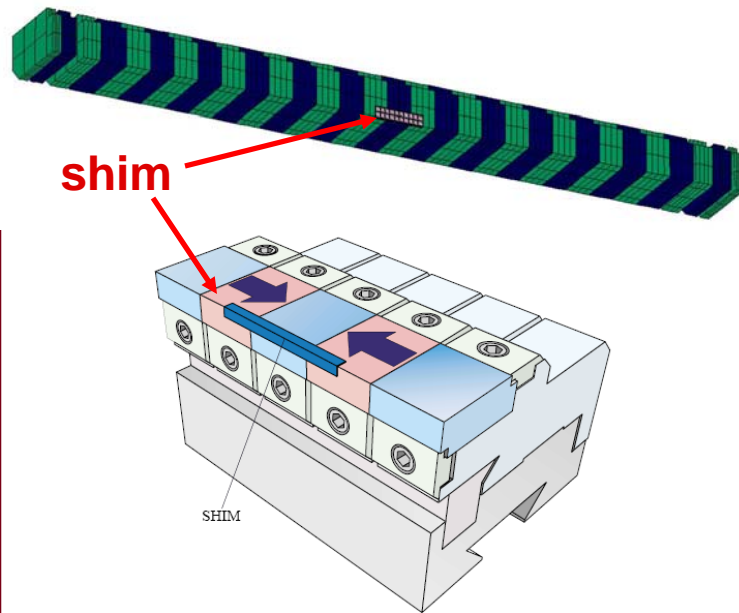- Dynamic aperture reduction induced injection losses

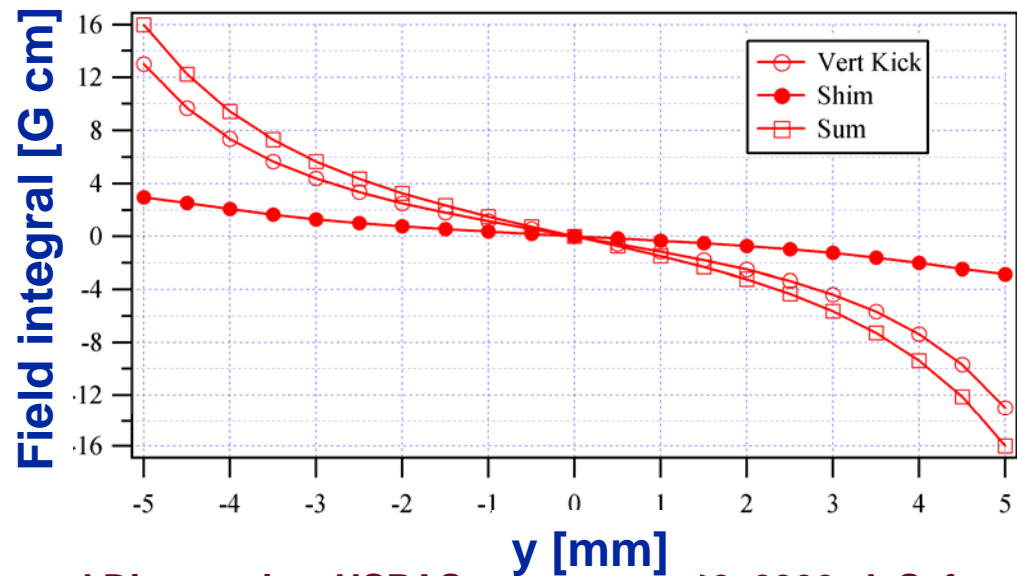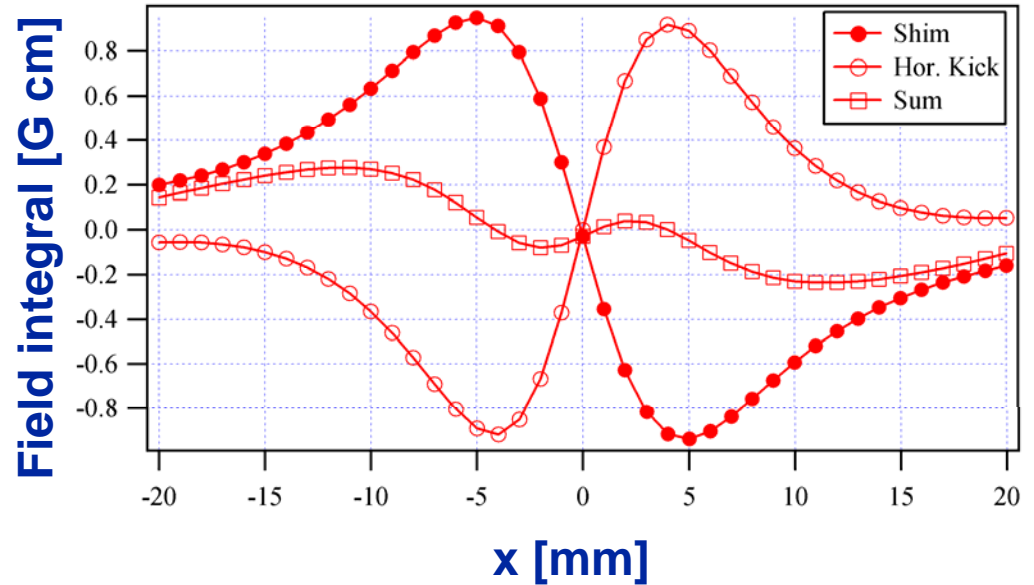**Vertical field** **Circular polarization** **Horizontal field**

Shims partially correct field integrals

shim

Shims correct field integrals in x-plane, but make integrals a bit worse in y-plane.
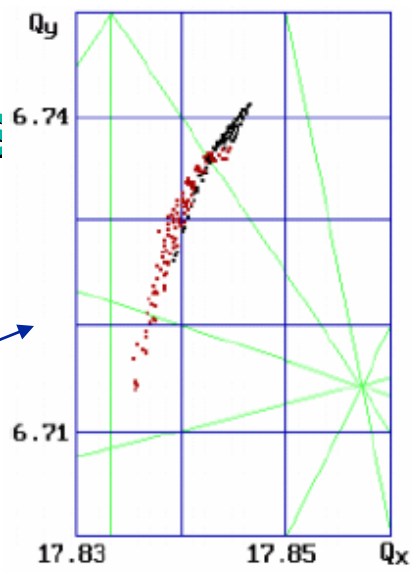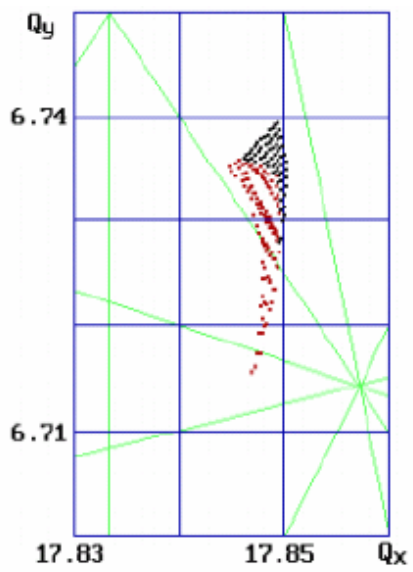
Overall beam dynamics improves.

BESSY II frequency maps with shims

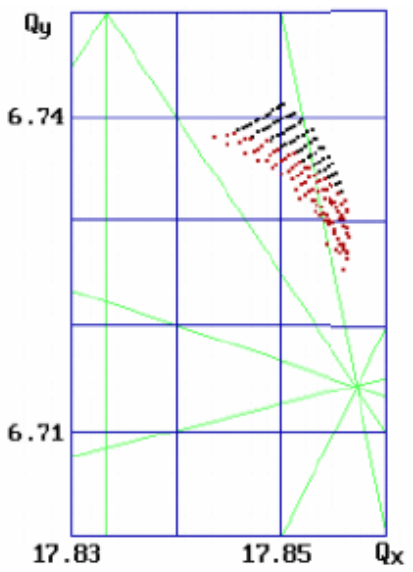○ **Before shims: Horizontal dynamic aperture and injection efficiency improved with shims.**
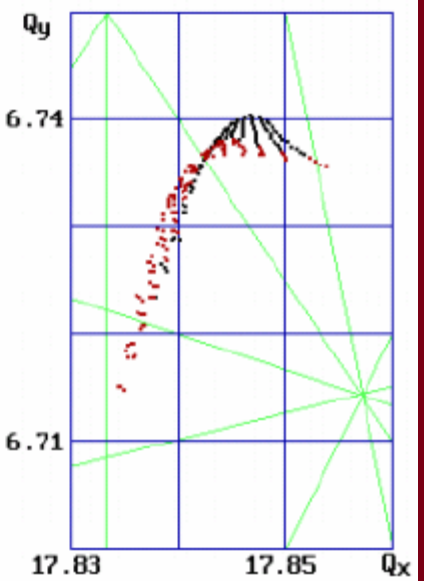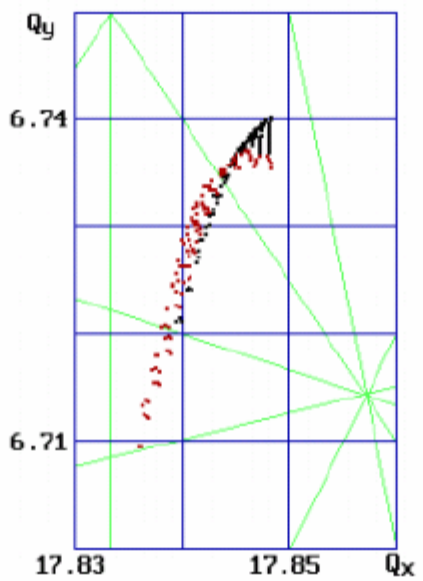
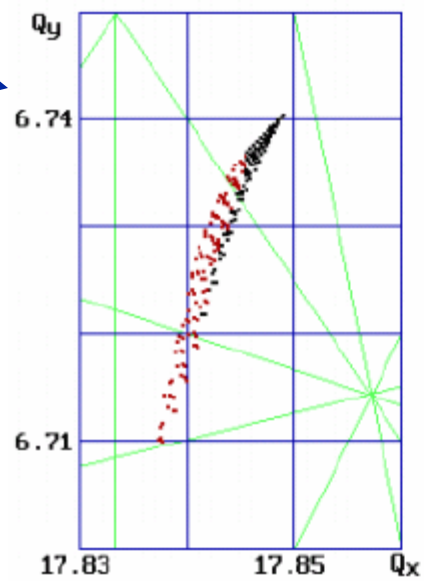○ **After shims: Vertical dynamic aperture decreased**

Vertical field

Circular polarization

Horizontal field

Selected further reading

Modeling wigglers:

    Weishi Wan, PAC03.

    David Sagan, PAC03.

    Ying Wu, PAC01 and PAC03.

    Elleaume, Pascal, "A new approach to the electron beam dynamics in undulators and wiggler", EPAC'92, page 661.

    Smith, Lloyd, "Effect of wigglers and undulators on beam dynamics", LBNL, ESG Technical Note No. 24, 1986.

EPU shims: J. Chavanne et al., "Recent achievements and future prospect of ID activities at the ESRF",   EPAC2000.

Beam-based measurements:

    Kuske, "Effects of fringe fields and insertion devices revealed through experimental frequency map analysis", PAC05.

    Temnykh, "CESR-C: Performance of a wiggler-dominated storage ring", PAC05

    Temnykh et al., "Beam based characterization of a new 7-pole superconducting wiggler at CESR", PAC05

    Steier et al, "Study of row phase dependent skew quadrupole fields in apple-II type EPUs at the ALS", EPAC2004.

    Temnykh et al., "Beam-based characterization of a new 7-pole super-conducting wiggler at CESR", PAC03.

    Kuske et al., "Investigation of non-linear beam dynamics with apple II-type undulators at Bessy II", PAC01.

    J. Safranek et al., "Nonlinear dynamics in a SPEAR wiggler", PRST-AB, Volume 5, (2002).

    Robin et al., "Global beta-beating compensation of the ALS W16 wiggler", PAC97.

Orbit control:

    O. Singh and S. Krinsky, "Orbit compensation for the time-varying elliptically polarized

    wiggler with switching frequency at 100 Hz.", PAC97.